Master's thesis

NTNU
Norwegian University of Science and Technology
Faculty of Information Technology and Electrical Engineering
Department of Electric Power Engineering

Ida Langseth

Voltage Support with Reactive Power from Fast Charging Stations with Local Energy Storage and Production

Master's thesis in Energy and Environmental Engineering
Supervisor: Jayaprakash Rajasekharan, Dept. of Electric Power Engineering
Co-supervisor: Jonatan Klemets and Bendik Nybakk Torsæter, SINTEF Energi AS
June 2021

NTNU
Kunnskap for en bedre verden

Ida Langseth

Voltage Support with Reactive Power from Fast Charging Stations with Local Energy Storage and Production

Master's thesis in Energy and Environmental Engineering
Supervisor: Jayaprakash Rajasekharan, Dept. of Electric Power Engineering
Co-supervisor: Jonatan Klemets and Bendik Nybakk Torsæter, SINTEF Energi AS
June 2021

Norwegian University of Science and Technology
Faculty of Information Technology and Electrical Engineering
Department of Electric Power Engineering

NTNU
Norwegian University of Science and Technology

Abstract

Norway is a world leader in electric mobility, and the Norwegian government has stated that all new passenger cars, light vans, and city buses should be zero-emission vehicles by 2025. Even though low power home charging is the most prevalent charging option today, the rapid increase in electric vehicles will also increase the need for fast charging stations that can compete with conventional fuelling stops. The associated high power of fast charging loads can lead to voltage issues, which is undesirable for the distribution grid operators. In this master's thesis, a methodology for voltage support from a fast charging station has been developed. Three control strategies namely, a rule-based, optimization-based, and a Model Predictive Control (MPC) based battery control have been developed, together with a reactive power control based on voltage sensitivity calculations. The purpose is to mitigate the voltage issues caused by high power charging, and simultaneously minimize energy costs for the charging station operator. To verify the proposed approach, simulations were carried out on a system consisting of a fast charging station equipped with 10 charging outlets of 150 kW rating each, a 1 MWh stationary battery, and a 1.38 MWp PV system. The control strategies are evaluated in a comparative analysis, and a sensitivity analysis is conducted.

The results demonstrate the benefits of a control strategy for reactive power and local storage- and production. The battery successfully minimizes energy costs for the charging station operator when an optimization-based control is used. Simultaneously, the voltage is corrected by reactive power injection. In a low production scenario, the rule-based control strategy does not utilize the full potential of the battery. With an optimization or MPC-based control, the battery recharges when the prices are low, which leads to new voltage drops. However, combined with reactive power, the voltage drop is mitigated. The reactive power is therefore the main contributor to the improved voltage profile. In a high production scenario, the results verify that the system can sustain an acceptable voltage profile. The battery and PV production are the main contributors to keeping the voltage close to the limit, and the main is that the optimal battery control can reduce costs to a larger extent than the rule-based control.

The sensitivity analysis demonstrates that an upper limit on the grid imported power or on the charging power, are possible solutions to the new voltage drops due to battery recharging. If the proposed battery controllers were to be implemented in practice, they should either account for grid tariffs or have an upper limit on charging power or grid imported power. It is also found that the proposed control system gives better voltage mitigation results with a 45% higher load, compared to the voltage without battery and PV and original load. The developed control strategy, therefore, allows higher charging powers for the charging station operators without causing significant grid impact. The results also illustrate that the utilization of reactive power can provide adequate voltage support even when the battery has a sub-optimal performance due to prediction errors for load and production, and could therefore allow less computationally expensive prediction algorithms.

It is concluded that the voltage at the critical bus can be improved considerably by using reactive power. By combining this with a stationary battery and local production, it can also increase benefit for the charging operator.

Sammendrag

Norge er ledende innen elektrisk mobilitet, og norske myndigheter har et mål om at alle passasjerbiler, lette varebiler og bybusser skal være nullutslippskjøretøy innen 2025. Med økt elbilandel vil også behovet for hurtigladestasjoner øke betydelig. Hurtigladestasjoner med høy effekt er viktig for å være konkurransedyktig mot tradisjonelle bensinstasjoner. Økte ladeeffekter fra hurtigladestasjonene kan medføre spenningsproblemer i distribusjonsnettet, som er uønsket for nettoperatørene. I denne masteroppgaven har en metode for å tilby spenningsstøtte fra en hurtigladestasjon blitt utviklet. Tre kontrollstrategier har blitt utviklet, en regelbasert, en optimeringsbasert og en Model Predictive Control (MPC) basert, sammen med en kontroll for reaktiv effekt basert på spenningssensitivitet. Hensikten er minske å spenningsproblemene som hurtiglading kan medføre, samtidig som kostnader for ladestasjonsoperatøren bli minimert. For å verifisere kontrollerne, ble disse simulert i en nettmodell, med et tilkoblet system som består av en hurtigladestasjon med 10 ladepunkter med 150 kW effekt hver, et 1 MWh stasjonært batteri og et 1.38 MWp solcellesystem. Kontrollstrategiene er evaluert i en komparativ analyse og en sensitivetsanalyse.

Resultatene demonstrerer fordelene med en kontrollstrategi for reaktiv effekt og lokal energilagring og produksjon. Batteriet minimerer energikostnadene for ladestasjonsoperatøren på en vellykket måte når en optimeringsbasert batterikontroll brukes, samtidig som spenningen korrigeres med injeksjon av reaktiv effekt. Med en optimeringsbasert og MPC-basert kontroll lades batteriet med effekt fra nettet når prisene er lave, som medfører nye spenningsfall. Imidlertid, hvis batterikontrollen er kombinert med kontroll for reaktiv effekt, reduseres disse spenningsfallene. Den reaktive effekten er derfor hovedbidragsyter til den forbedrede spenningsprofilen. I et scenario med høy produksjon, viser resultatene at systemet er i stand til å opprettholde en akseptabel spenningsprofil. Batteriet og PV-produksjonen er de viktigste bidragsyterne til å holde spenningen nær grensen. Hovedforskjellen er at den optimeringsbaserte batterikontrolleren er i stand til å redusere kostnadene i større grad enn den regelbaserte kontrolleren.

Sensitivitetsanalysen viser at en øvre grense på nettimportert effekt eller ladeeffekt er mulige løsninger på de nye spenningsfallene som følge av batteriladingen. Hvis de foreslåtte batterikontrollene skulle ha blitt implementert i praksis, bør de ta hensyn til nettleie, eller ha en øvre grense for batterieffekt eller nettimportert effekt. Det er også funnet at det foreslåtte kontrollsystemet gir bedre spenningsresultater med en 45% høyere last, sammenlignet med spenningen uten batteri og PV med den opprinnelige lasten. Den utviklede kontrollstrategien tillater derfor høyere ladeeffekter for ladestasjonen uten å forårsake økt nettpåvirkning. Resultatene illustrerer også at bruken av reaktiv effekt er i stand til å gi tilstrekkelig spenningsstøtte selv når batterier har suboptimal ytelse grunnet avvik i prediksjoner for last og produksjon, og kan derfor tillate mindre avanserte prediksjons-algoritmer.

Det konkluderes med at spenningen ved den kritiske bussen kan forbedres betraktelig ved å bruke reaktiv effekt. Ved å kombinere dette med et stasjonært batteri og lokal produksjon, kan det også øke fordelen for ladestasjonsoperatøren.

Preface

This thesis is submitted as the final part of the 2-year master's degree in Energy and Environmental Engineering for the Department of Electric Power Engineering at The Norwegian University of Science and Technology, spring 2021. This report is written in collaboration with and is a part of KPN FuChar. FuChar is a KPN project funded by The Research Council of Norway and industry partners. The FuChar project aims to minimize investment and operating costs related to the grid integration of electric transport, focusing on fast charging.

Bendik Nybakk Torsæter and Jonatan Klemets at SINTEF Energy Research deserve sincere thanks for contributing to the thesis with valuable inputs, guidance and data, and for letting me be a part of the FuChar project. I would also like to express great gratitude to my primary supervisor Jayaprakash Rajasekharan for his excellent advice and support throughout the semester.

Trondheim, 14.06.2021

Ida Langseth

Ida Erika Witt Langseth
476031

Contents

Abbreviations

BEV	Battery Electric Vehicle
CCS	Combined Charging System
DSO	Distribution System Operator
EV	Electric Vehicle
FCS	Fast Charging Station
MILP	Mixed-Integer Linear Programming
MPC	Model Predictive Control
PV	Photovoltaic
SOC	State of Charge
TSO	Transmission System Operator
V2G	Vehicle-to-Grid

List of Tables

List of Figures

Chapter 1

Introduction

1.1 Background

As the global economy and population are growing, so is the energy demand and the subsequent greenhouse gas (GHG) emissions, and there is a need for new technologies and intelligent solutions to meet the demand. The electricity demand is estimated to double from the year 2019 to 2050, which is a result of a combination of electrification of existing energy use, as well as population growth and increased standard of living [1]. In 2019, the transport sector amounted to 27% of the world's CO_2 emissions. Electrification of the transport sector is, therefore, a great step towards the reduction of GHG emissions, if the electricity comes from renewable sources. The global electric vehicle (EV) market has expanded significantly in the last 10 years. To put it in context, the world's battery electric vehicle (BEV) stock has increased from 0.02 million to 4.69 million from 2010-2019. 17 countries have stated zero-emission vehicle goals for 2050, including Norway [2]. As half of the emissions from the transport sector originate from road transport, the National Transport Plan states that all new passenger cars, light vans, and city buses should be zero-emission vehicles by 2025 [3]. Zero-emission vehicles comprise vehicles that have no tailpipe emissions, such as EVs. In addition, EVs charging from the Norwegian distribution grid are charged with renewable power. This indicates that electrification of the transport sector will be an important step towards reaching the national climate goals [3]. There is a need for sufficient infrastructure and facilitation to supply the required amount of energy.

1.2 Motivation

As a consequence of the growing EV sales, the demand for public fast charging is bound to increase to be able to compete with conventional fuelling stations. By the end of 2020, there were 3270 public charging points on the Norwegian roads that offer high power charging [4]. The Norwegian EV association estimates that to meet the future demand, 1250 fast chargers need to be built every year towards 2025 [5]. The aggregated load of fast charging stations (FCS) might lead to capacity issues in the distribution grid, such as voltage drops, transformer overloading, and harmonics [6]. For grid operators, the increased high power charging therefore poses a challenge, especially when it comes to long-term planning and grid investments. It is not economically efficient to dimension the grid for the peak loads of FCS. However, increased electrical load from EV adoption is also a good opportunity to invest in flexible resources and control systems to manage high peak loads and augment the hosting capacity of the distribution grid. The expected increase in FCS load is also an opportunity to investigate new ways that the FCS can support the grid, both by limiting high load peaks or by providing services, such as voltage support, to the grid operator. A typical example is when the distribution system operator (DSO) is interested in keeping the voltage at an acceptable level and postponing investments to reinforce the grid. Possible solutions to this are by utilizing flexible resources on the demand side, for example by peak load curtailment or voltage support with reactive power.

When it comes to charging station operators, the goal is to maximize the revenues from charging vehicles. It is therefore unfavorable to limit the customers charging power to reduce grid impacts. Grid services are

therefore especially relevant for FCS operators, as they could potentially allow the charging powers, or the number of charging outlets, to increase. Potential grid services that FCS could provide is for example by using local storage or production to respectively reduce peak loads or increase self-consumption.

The topic of limiting grid impact of EV charging by local storage or production has been extensively researched [7–9]. There is existing research on smart charging and charging stations providing grid services [10–14]. There is also research on using batteries and local production for maximizing self-consumption and reducing voltage variations [15–17]. In [10], a Model Predictive Control (MPC) was developed that coordinated the reactive power among different chargers at an FCS to improve the voltage profile for the grid, however, no additional components to increase FCS operator benefit were included. There is a research gap when it comes to the combined interests of charging station- and distribution grid operators. Providing grid services could potentially increase the capacity of the charging station, which could yield increased profits. It is also an important success factor for the Norwegian government in the goal towards zero-emission vehicles. There is a need for new control strategies, management systems, and increased interaction between the charging station, vehicle, and the grid to achieve this. The goals, problems, and possible solutions are summarized in Figure 1.1.

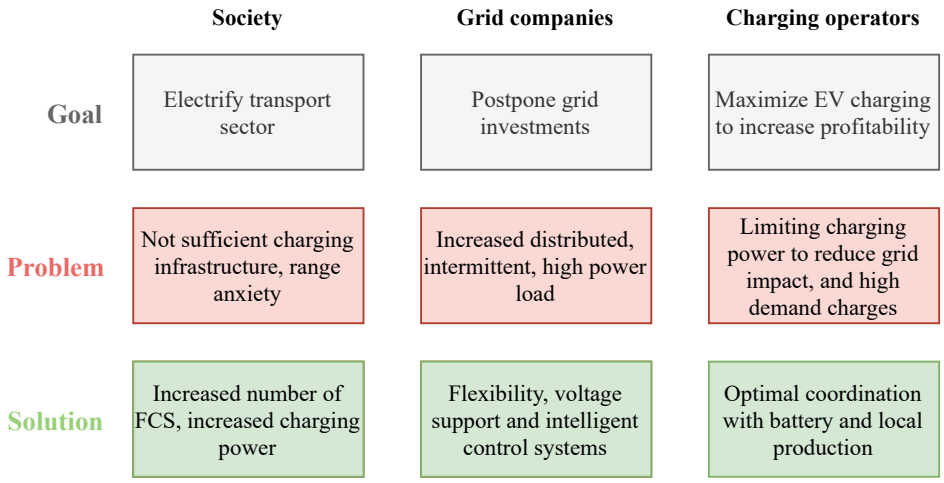

Figure 1.1: The main goals for this thesis, along with associated challenges and possible solutions. The thesis addresses each of the three goals, and contributes by proposing a methodology to help the stakeholders towards their goals.

1.3 Scope of Thesis

There is a gap in existing research when it comes to combining the interests of charging station operators and distribution grid operators. One aspect of this problem is load modeling and providing a management system for the components at the FCS to meet the goal of the operator, which could be for example maximize self-consumption or minimize cost. The second aspect concerns the potential services that the FCS can provide the grid, especially voltage support through reactive power. It is necessary to have a sufficient energy management system as a foundation when exploring how the FCS can provide grid services. An energy management system was developed for the FCS in a specialization project [18] that preceded this thesis work. This thesis comprises the second aspect of the problem, which is to investigate the services the FCS can provide to the distribution grid. To achieve this, this thesis, therefore, focuses on the second aspect of

the problem - to investigate voltage support services that can be provided by the FCS in combination with batteries and a photovoltaic (PV) system. The optimal operation between the fast chargers, battery, and PV, to benefit both the FCS operator and the DSO, is investigated.

The objective of this thesis is to design a new methodology for combining the interests of the FCS operator and the DSO, by simultaneously minimizing energy costs and providing voltage support through reactive power. This is realized through a control system applied to critical buses in the distribution grid, to optimize the coordination between the FCS, a PV system, and a stationary battery. The following questions will be addressed:

- What is the optimal battery control strategy for the charging system operator? How can variation in inputs such as load and prediction, battery power limit and grid power limit impact the optimal operation of the system?
- What is the optimal strategy to utilize reactive power to limit grid impacts of a fast charging station?
- How can a combined control strategy for reactive power and local storage and production benefit the charging station- and grid operator?

To address the research questions, three battery controllers will be designed. The controllers are: one rule-based control and one Mixed Integer Linear Programming (MILP) based control with deterministic power predictions, and one based on Model Predictive Control (MPC) with non-deterministic power predictions. Deterministic input means that the production- and load predictions are perfect and known. Non-deterministic inputs refer to when the predictions are imperfect, and there are deviations between predicted and measured power. The MPC-based controller will demonstrate an approach to deal with prediction errors in load and production.

A controller for reactive power based on voltage sensitivity calculations will also be designed and should ensure that the voltage is within acceptable limits. To verify the controllers, the controllers will be simulated in a grid model, which contains an FCS load, PV system, and stationary battery. The simulations will be done in a model of the Norwegian distribution grid Stange. The operational strategies will be tested in the grid model under different operational scenarios and a comparative analysis of the strategies will be made. Here, the controller with deterministic inputs will be compared, and they will not be directly compared to the MPC-control as it is tested on different inputs. To get a deeper insight into the results, a sensitivity analysis will also be provided.

1.4 Contributions

This master's thesis is a part of the research project FuChar, lead by SINTEF Energy Research. The project aims to minimize investment and operating costs related to grid integration of electric transport. The research topics for the FuChar project are:

- Analysis of transport patterns, user behavior, and charging profiles from electric vehicles and vessels
- Development and testing of alternative system configurations and control systems for increasing utilization of flexibility in charging infrastructure

- Development of methods for optimal planning and operation of charging infrastructure in the distribution grid

The project partners hold broad competence and include both grid companies and charging infrastructure operators. The partners involved in the FuChar project are Agder Energi Nett, Elvia, Haugaland Kraft Nett, IONITY, Istad Nett, The Norwegian Electric Vehicle Association, NVE, Skagerak Nett, Norwegian Public Roads Administration, SINTEF Community, NTNU, and UPC [19]. This thesis is contributing to the activity concerning charging technology and flexibility. The contributions of this thesis to the FuChar project is summarized below:

- Three battery control strategies, which together with a PV system can be operated to minimize cost for the charging station operator.
- A reactive power controller based on voltage sensitivity calculations which can be used as voltage support from the FCS alone or in conjunction with a battery and PV system.

The developed control algorithms, which optimize both active and reactive power flow, can be useful for the entire system, both distribution system operator and charging operator.

1.5 Thesis Outline

The content of the remaining chapters is the following: *Chapter 2, Theory and Background*, presents the theoretical foundation and literature for the thesis. It provides the context for the modeling and discussion, as well as a mathematical description of the modeling theory. *Chapter 3, System Description*, describes the system used in the simulations. *Chapter 4, Methodology*, gives a detailed description of the methodology used in the simulations, including grid- and controller modeling. *Chapter 5, Results*, presents the results, including operational results from three different operational scenarios as well as a sensitivity analysis. *Chapter 6, Discussion*, discusses and provides insights on the operational results and modeling. Recommendations for further work are also suggested. *Chapter 7, Conclusion and Further Work*, concludes on the research questions in the introduction.

Chapter 2

Theory and Background

This chapter provides the theoretical foundation for the thesis and associated literature review. State-of-the-art charging technology is presented. Insights on the electricity grid including voltage issues and possible solutions through ancillary services are also provided. Different sources of ancillary service provision - from EVs and chargers, stationary batteries, and local production are presented. The purpose of the three first sections is to provide the context for the modeling and discussion.

The final section constitutes a mathematical description of the modeling. This includes grid modeling, voltage sensitivity, and control theory. The latter aims to clarify the concept and literature on the control strategies used in this thesis, which as mentioned in the introduction, is a rule-based, optimization-based, and MPC-based control.

2.1 Electric Vehicle Charging Technology

Today's charging methods can be divided into three categories: conductive charging, inductive charging, and battery swapping. The most common charging method is conductive charging, which is charging the car battery with electrical conduction through a socket. Inductive charging uses electromagnetic fields to charge the battery and is often referred to as wireless charging. The last method is battery swapping, which is physically switching the battery of the car with a fully charged battery. As conductive charging is the most prevalent charging method today, this is the focus of this thesis. There are three main charging levels for conductive EV charging. They are presented in Table 2.1.

Table 2.1: Charging levels for EVs [20–22]. Level 4 and 5 are not standard names for the levels, and are therefore written in italics.

Power levels	**Level 1**	**Level 2**	**Level 3**	***Level 4***	***Level 5***
Power Range	$\leq$ 3.7 kW	2.7-22 kW	$\geq$50 kW	$\geq$150 kW	350 kW
Charging time	11-36 h	1-6 h	0.2 - 1 h	0.1-0.4 h	Minutes
Charger topology	On-board	On-board	Off-board	Off-board	Off-board
Charging type	Slow charge	Semi-fast charge	Fast charge	Fast charge	(Ultra) fast charge
Typical location	Households	Mall, workplace	Highway, stores	Highway	Highway

As mentioned in Table 2.1, level 3 allows charging over 50 kW and is classified as fast charging. The accumulated load at an FCS with multiple charging points can therefore be high. It is also shown that level 2 charging, which is up to 22 kW, can cause an impact on the distribution system even with low EV penetration. The accumulated load at a specific area may cause power losses, power quality problems, transformer degradation, and other unwanted phenomena [23].

There are two standard charging interfaces: CHAdeMO and Combined Charging System (CCS). In addition, Tesla has developed their own Tesla Supercharger which is available exclusively for Tesla users. The CCS interface provides higher possible charging power, and new vehicles equipped with CCS theoretically can reach up to 350 kW. At this charging level, it can be comparable to conventional fuelling stops. The Tesla V3 Supercharger can deliver charging rates up to 250 kW, leading to a charging time of 15 minutes to reach 80% state of charge (SOC) [24]. Even though CCS currently can reach a higher power, CHAdeMO released the CHAdeMO 3.0 protocol in 2020, which enables DC charging power of 500 kW [25]. In a competitive market, it is clear that the trend is to implement ultra-high charging powers. However, the bottleneck for ultra-high charging capacities is excess heat in the batteries, limited charging rates in the battery cells and large currents in the charging connector [7]. Not all cars on the market can charge at this rate, but the maximum charging rates are increasing. Therefore, the challenges of fast charging are different from the challenges of slow charging, as they have short charging periods of high power and varying arrival rates at the charging station.

Charger Configuration

Fast charging is realized through power electronics located outside the EV and is generally referred to as off-board chargers. This can be seen from Figure 2.1, where the configuration to the right shows the off-board charger and related charging interfaces. Fast charging usually does not apply to households because there are limitations due to the rating of low-voltage grid connection cables. Charging levels 1 and 2 are the most relevant for households, and their configurations are presented in Figure 2.1 respectively the first and second to the left.

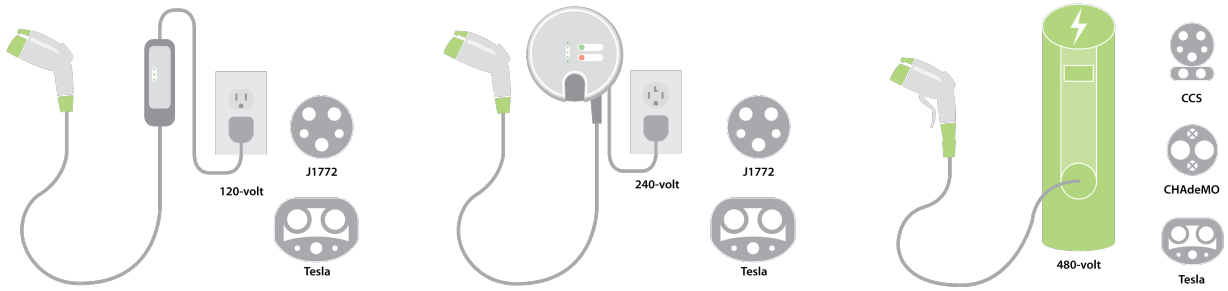

Figure 2.1: Charging levels and their configurations. From left to right, the charging levels are Level 1, Level 2, and Level 3. Levels 1 and 2 are relevant for households, and level 2 is also used at many public charging stations. Level 3 exceeds the low voltage grid rating and is more relevant for medium voltage grid connections, for example along the highway [26].

The car battery is charged by DC power while the power supplied by the grid is AC, and an AC/DC converter is therefore needed. Every vehicle has an onboard charger, which allows AC/DC conversion when connected to level 1 or 2 chargers. For level 3 charging, the configuration is a little different. The AC/DC conversion happens off-board, and the socket charges the battery directly with DC power [23].

2.2 The Norwegian Electricity Grid

The Norwegian electricity grid consists of three sub-levels, which determine the voltage level and operator. The transmission grid has a 300 or 420 kV voltage level, and connects producers and consumers over far distances both domestic and overseas, enabling power import and export. It is operated by the transmission system operator (TSO), Statnett. The regional grid connects the transmission- and distribution grid and the voltage level is 132 or 66 kV. The distribution grid supplies the end-users and includes voltages from 22 kV to 230 V. Consumers are connected to the distribution grid, with transformers to step the voltage down to lower voltage levels. The distribution grid is operated by the DSO, which is responsible for the grid in a geographic area [27].

Grid operators are regulated, as they are natural monopolists. The regulation is in place to ensure that operation, utilization, and development of the electricity system is in the society's best interest [27, 28]. In Norway, the Norwegian Water Resources and Energy Directorate (NVE) is regulating the grid operation. A part of this is securing the voltage to be kept within certain levels. In the regulation concerning power quality, the limits of different voltage phenomena are defined. For slow voltage variations, as described above, it is stated that: "*Network companies shall ensure that slow variations in the effective value of the voltage are within a range of* ± 10 *% of nominal voltage, measured as an average over one minute, at the*

connection point in the low-voltage network [1]. Voltage phenomena can happen in the distribution grids for numerous reasons, for example as a result of changes in load and production. Figure 2.2 shows the effect of light and heavy load on the 22 kV grid, and low voltage grid. A tap changing transformer is used to correct the voltage at the substation.

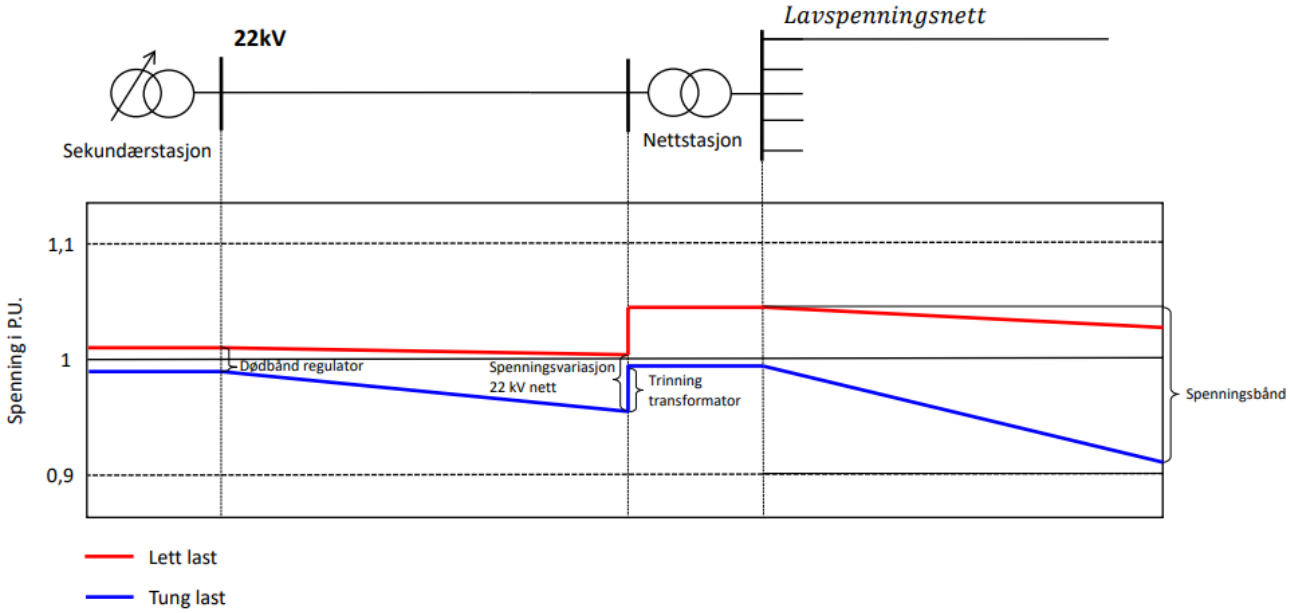

Figure 2.2: Slow voltage variations in the distribution grid with light (red) and heavy (blue) load. [29]

An overview of the grid impact of slow and fast charging has been analyzed in [30]. The impacts include voltage imbalances, voltage deviations, line and equipment overloading, supply-demand imbalances, and instability problems. The impact of fast charging on the grid is investigated in [6], where it is underlined that the impact of fast charging in distribution networks is considerable, especially when the charging is done in a congested distribution network. This will then lead to peak loads, harmonics, and low power factor. Solutions proposed to this issue are an additional energy storage system, e.g., a stationary battery, and thus shifting the load to a less congested time of the day. Uncoordinated charging has a considerable impact on peak load, losses, voltage, etc., and reduces the overall efficiency of the distribution grid [31]. Also, [32] showed the impact of coordinated charging in a 10 % EV penetration scenario, where the uncoordinated case caused unacceptable voltage variations, while the coordinated case leads to reduced peak load, losses, and overall mitigation of the impact on the distribution system.

Electricity prices

Electricity consumers pay for both the electricity price to their electricity supplier and grid tariffs to the local grid operator. Grid tariff should reflect the operating costs of the grid. When it comes to the electricity price, there is a market-based price formation to ensure that the demand is satisfied at the lowest possible cost to society. The electricity market is operated by Nord Pool. The day ahead prices are based on the

[1] Forskrift om leveringskvalitet i kraftsystemet § 3-3

supply-demand principle. Consumers and producers place bids before noon the day-ahead, and the prices are set for all 24 hours of the next day. The aggregated supply and demand are put into two curves. The price is set where the supply meets the demand and is referred to as the spot price. The price can be an indicator of the grid capacity, as the price goes up when the demand is high. However, price signals alone are not able to reflect grid issues, as many other factors impact the prices, such as weather, fuel costs, precipitation, or availability of generation resources [33].

The other part of the electricity bill for the end-users is the grid tariff. The grid tariff is paid to the local grid operator and should reflect the operating costs for the grid. In many cases, the grid tariff consists of a fixed and variable component. The variable component should equal the short-term marginal costs of their usage, in addition to the transmission losses if the customer is supplied from the transmission and regional grid or feed electricity to the distribution grid. In addition to the variable components, customers also have to pay a fixed component, which covers customer-specific costs. A capacity charge is also charged for capacity metered customers. This component is usually decided based on the peak hour of the month [28]. From an FCS perspective, it can be discussed if the design of the capacity charge is reasonable, and it could lead to less profitability for the FCS operator due to irregular demand. However, this issue has been addressed by NVE. It was suggested that it is fairer to bill the capacity charge based on the daily peak, compared to the monthly peak [34].

Unlike active power, there are no markets for reactive power as of today. However, there has been researched on different approaches to price-setting the reactive power. In [17], the effects on reactive power injection of PV inverters of the lifetime reduction have been quantified. This is done as an increase in the levelized cost of energy, which is translated into reactive power cost. The reactive power price is the active power price multiplied with the additional power loss in the inverter because of the injection, in addition to a lifetime reduction term. The authors in [35] have a market-based approach, which includes a new optimization model for pricing based on distributional locational marginal prices. [36] proposes a method for calculating short-run marginal costs, composed of network losses, voltage violation, and reactive power limit violation costs. The results show that the short-run marginal costs are dominated by the network loss component, and the voltage control-related cost is relatively small. [37] provide a programming method to obtain a spot/real-time pricing, showing the effects of various factors on reactive power marginal price.

2.3 Ancillary Services

Provision of ancillary services is necessary for a distribution grid with increased penetration of DER and connected loads such as FCS. They can take the form of operational management, frequency control, voltage control, and system restoration [38]. Ancillary service products range from operating resources from grid operators to power generating plants and flexible loads. In this context, end-user batteries become attractive, as is it acts as both a generating and consuming unit. Managing the flexible loads and units situated at the demand side is referred to as demand-side management (DSM). DSM can lead to reduced grid impact from the DER. Examples of DSM are load shifting, peak clipping, strategic conservation and valley filling [16]. The different concepts are illustrated in Figure 2.3.

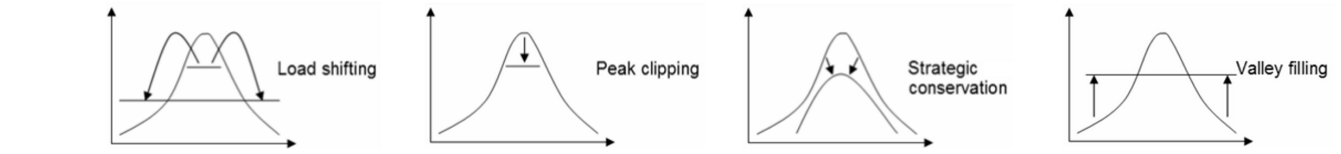

Figure 2.3: The different types of demand-side management, load shifting, peak clipping/shaving, strategic conservation and valley filling [16].

Another way to provide ancillary services is through reactive power support. This is done by power electronic generation of reactive power in converters, which can be injected or absorbed from the grid, as a response to voltage limit violations. Traditionally, this is done by for example switchable capacitor banks and on-load tap changers. Due to an increase in distributed generation, centralized generation can lead to excessive tapping of on-load tap changers. However, with an on-site generation of reactive power, there is less need for transmission of generation-side reactive power. This reduces losses in the distribution system, and prevents overloading of distribution transformers [39]. The following subsections will provide information about examples of different components that can provide ancillary services: EVs and chargers, stationary batteries, and PV systems.

2.3.1 Provision from Electric Vehicles and Chargers

When it comes to charging stations, off-board battery chargers can support the grid by injecting reactive power if the charger is equipped with a bi-directional converter. Reactive power injection is done without impacting the charging of active power to the battery, which is ideal for an FCS, as the main goal is to charge in the shortest possible time [12]. This also leads to less deterioration of the battery, as compared to using active power. Therefore, voltage drop issues due to EV fast charging can be managed using a reactive power supply without limiting the active power or causing unnecessary degradation of the car batteries. The challenge with utilizing EV chargers as reactive power support is that the amount of reactive power supplied is limited by the charger rating. Often, when the active power is high, the need for reactive power is also high, thereby reducing the amount of reactive power available. It is demonstrated that the DSO could issue higher upper bounds on the active power limits for EVs if the FCS injects reactive power, under the same grid conditions. In other words, the capacity of high power charging is increased if FCS injects reactive power [13]. [13] also finds that coordinated charging significantly reduces the average cost of EV charging if it takes place in the fourth P-Q quadrant.

There is also some existing research on ancillary services provision from FCS, using frequency regulation [11, 14]. [11] presents the impact that FCS has on power system operation in a system that provides reserves for frequency regulation. The system consists of RES, conventional power plants, and FCS. [14] presents a concept where a charging station for electric buses is used for secondary frequency control using a storage system. Most of the research concerning ancillary services from FCS includes additional components, such as a stationary battery.

Electric vehicles can also be used to provide ancillary services through Vehicle-to-Grid (V2G). The concept of V2G is when there is controllable and bidirectional electrical energy flow between a vehicle and the

electrical grid [23]. The car batteries and battery chargers can be used to serve electricity markets, as EVs are not being used for transportation 90% of the time. The main benefits of V2G are peak load leveling, the financial benefit for EV owners, renewable energy storage, and possible support during a power outage. However, V2G technology is also subject to certain risks. Examples of risks are costs of power electronics due to bi-directional interface, battery life reduction, modeling complexity, and market risk. As a result, the economic benefit is still in question. There are different perspectives on the economic benefit in the research community. [40] investigate the EV owners' benefit, and the charging scheme is based on the electricity price. The consumer benefit is mainly from saving money on charging during non-peak hours when the price is low and discharging when the price is high. [41] compares the benefit of EV users, grid companies, and power generation companies of V2G as a peak shaving service and concludes that the power generation companies are the primary beneficiaries of the V2G mode in this case. Additionally, the use of V2G mode is more relevant in a residential charging situation than for FCS, because the battery is connected for a longer period. For an FCS, the goal is to charge as fast as possible, which conflicts with the V2G principle.

2.3.2 Provision from Stationary Batteries

Batteries in the distribution grid, stationary or mobile, can provide services to the grid, for example by load shifting, which is using batteries to supply loads during peak price hours, and charging the battery when the prices are low [15, 16]. Stationary batteries are an important resource for the future power system, they have the potential to provide multiple services. Potential services can be for example buffer for local production, frequency control, voltage control, or DSM as illustrated in Figure 2.3. This creates value for the grid operators, as the use of batteries can act as an alternative to grid reinforcement. What makes the battery so favorable is that it can provide multiple services simultaneously, increasing the benefit for the investor. In addition to projected significant price reductions for battery technology, intelligent control strategies can also maximize the services the battery can provide, making a battery investment even more beneficial. The National Renewable Energy Laboratory projected the battery costs for utility-scale Li-ion batteries until 2050, and the results are presented in Figure 2.4.

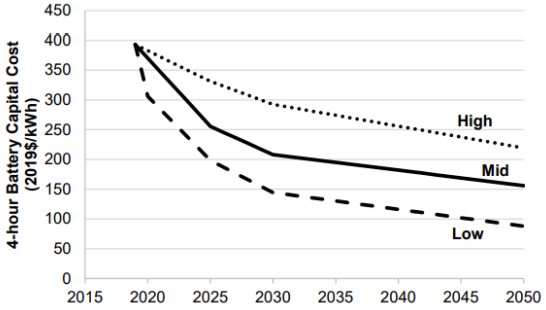

Figure 2.4: Battery cost projections (high, mid and low cost) for utility scale Li-ion batteries. Even with a high cost projection, the battery costs will be halved by 2050, and with a low cost projection, the price per kWh will be 25% of what it was in 2020 [42].

Consumption at an FCS can have high peaks. An energy storage system, e.g. a stationary battery, might be used for peak shaving [7]. Batteries can also provide voltage support, both through reactive- and active power. Voltage support with reactive power entails that the converters connected to batteries can help to

keep the voltage within an acceptable range by injecting reactive power when the voltage is low or absorbing reactive power when the voltage is high. The activation of this service is by slow voltage variations caused by changes in load or production. This solution has no direct market effect, but it has the potential to reduce transmission losses. On the other hand, voltage support with active power is used for fast voltage variations, thus having a market effect [15].

In an analysis, the role of the consumer benefit of on-site batteries is emphasized [9]. In this analysis, the capacity charge (the grid tariff component based on the peak power) constitutes around 90% of the monthly electricity bill for the charging station. With a storage system, the capacity charges are reduced by 73%, which reduces the EV drivers' cost as well. The use of batteries for multiple services such as frequency regulation and demand response is also emphasized. In [8], it has been found that the use of on-site batteries at fast charging stations is economically efficient, however, the efficiency depends strongly on the avoided electricity costs, additional revenues, and battery cost. It is concluded that a way to increase the economic benefit of the battery is the battery could participate in other markets such as the intraday market or as a frequency response reserve.

The price elasticity of charging demand can be used for load shifting or peak shaving. If the demand is price elastic, it means EV drivers will either reduce the charging time or power due to high prices or choose to charge at another time of the day when the prices are lower. With such behavior among EV drivers, different grid tariff structures might be an incentive for the customers to have flexible loads. [43] found out that with EV consumer flexibility, charging during off-peak hours, the need for an energy storage system reduces. However, it is also emphasized that planning an FCS assuming flexible charging times is risky for the charging operator because they rely on the consumers to control the cost outcome.

2.3.3 Provision from Photovoltaic Systems

There are also benefits from having local production at the FCS site, as it could reduce costs for the customer by increasing self-consumption, and reduce power peaks for the DSO. PV technology has had a sharp decrease in manufacturing costs, which has made PV generation increasingly attractive. This is reflected in the global installed capacity of PV modules, which has had significant growth since 2000 [44]. The costs are expected to continue to decrease towards 2050. As the produced power from PV systems is DC, there is a need for DC/AC inverter to be able to supply the produced power to AC appliances or the distribution grid. This is the main objective of the PV inverter, but the inverter-based PV system is also able to generate reactive power. This can contribute to keeping the voltage and frequency within a specified range. Due to the growth of distributed PV generation, there is a lot of potentials for the PV inverters to provide ancillary services.

Reactive power support from PV inverters has proven to reduce losses, decrease line loading, maintain system voltage and reduce the overall cost of running the distribution grid [17]. Even though there are no direct costs of generating reactive power through the inverter, there are trade-offs that need to be considered. PV inverter losses increase when reactive power is being generated, which is an indirect cost. In addition, varying the power factor of the inverter can lead to stability issues by total harmonic distortion. The additional wear on the inverter has been shown to reduce the lifetime of the inverter [17]. The lifetime reduction can be translated to a cost for the PV system owner. The advantage of using PV inverters for reactive power

support in contrast to traditional approaches such as capacitor banks is that they are already accessible, and there is no additional investment [17]. Solar-powered charging stations are an important way to promote EVs. This is because it leads to self-consumption and therefore reduction of peak power drawn from the grid and reduced losses as the power is generated locally. In addition, installing solar power at the FCS increases the environmental benefit, especially in countries where the majority of the power production is from non-renewables. This promotes the image and perception of using EVs.

A PV system or charging station could also provide services to the DSO directly, by contributing with up or down-regulation of active or reactive power, upon request from the DSO. Having a limitation of FCS load is not advantageous because the main purpose of the station is to provide the highest power possible, to reduce the charging time. Utilizing local generation could therefore create value for both the customer and DSO.

2.4 Modeling Theory

This section describes the theory used in the modeling part of the thesis. Grid modeling is explained by elaborating on load flow analysis and mathematical representation of the power system. The theoretical foundation for reactive power calculations using voltage sensitivity is provided. The explained concepts are used as a basis for the grid modeling in the main part of the thesis. Further, the control theory is provided. This includes concept and literature on the control strategies used in this thesis, which is a rule-based, optimization-based using a MILP problem, and MPC.

2.4.1 Electricity Grid Modeling

The power system, or parts of the power system, can be represented as transmission lines, buses, generators, and loads. Load flow analysis is a solution for the network that shows the distribution of current, voltage and power flows at every bus in the system [45]. Load flow is a fundamental concept in power system theory, and the main goal is to find a feasible load flow in a network, keeping the voltage profile for all the buses within acceptable limits [46].

The inputs of the load flow analysis are bus data, line data, and generator/load data. The output is voltage magnitude and angles, real and reactive power, current flow, and power losses [47]. The buses in the power system can be classified into three types as presented in Table 2.2.

Table 2.2: Classification of buses. They are divided into three classes, with different data inputs and unknown variables [46].

Bus type	Data inputs	Unknown variables
Slack	V, δ	P, Q
PQ (load bus)	P, Q	V, δ
PV (generator bus)	P, V	δ, Q

V and δ are voltage magnitude and angle respectively. P is reactive power and Q is active power. It can be seen that for a slack bus, the voltage variables are known, V and δ. Usually, the slack bus is denoted the reference bus, as all the other buses in the system have variables in reference to the slack bus. Therefore, the voltage magnitude and angle are usually 1 pu in magnitude and 0°in angle. The active and reactive power at the slack bus is used to balance the system [46].

The PV bus has a voltage source connected, e.g. a generator, and the PV bus, therefore, has voltage control capabilities. The PV bus often has a load connected, however, it could also be classified as a PQ bus if it is a generator without voltage control capabilities connected. In that case, the generator is represented as a negative load [46].

Mathematical formulation

Both the line and transformer parameters are constant in the power system. With this consideration, the power system network is linear. However, there is a non-linear relationship between current and voltages at the bus, and this means that the power flow calculations at each bus involve solving non-linear equations [45]. There are different ways to mathematically model and solve the power flow. Common approaches are for example the Newton-Raphson method, Gauss-Seidel method, or DC power flow. All the methods contain linearization of the equations, either around an operating point or of the entire system. The power system equations are presented in 2.1 and 2.2.

$$P_i = V_i \sum_{j=i}^{n} V_j (G_{ij} cos\theta_i + B_{ij} sin\theta_{ij}) \tag{2.1}$$

$$Q_i = V_i \sum_{j=i}^{n} V_j (G_{ij} sin\theta_i - B_{ij} cos\theta_{ij}) \tag{2.2}$$

P_i is the active power, Q is the reactive power, G is the conductance, B is the susceptance, V is the voltage magnitude, θ is the voltage angle, and the i and j subscripts denote which bus it is. A power flow equation is formulated for each of the unknown variables for each bus. One of the key parts of the power flow analysis is the Jacobian matrix. It is a sparse matrix that is the basis for power flow calculations, containing partial derivatives of P and Q with respect to δ and V. It contains four submatrices that describe the relationship between the four different variables.

$$J = \left[\begin{array}{c|c} J_{P\delta} & J_{PV} \\ \hline J_{Q\delta} & J_{QV} \end{array}\right] = \left[\begin{array}{ccc|ccc} \frac{\partial P_2}{\partial \delta_2} & \cdots & \frac{\partial P_2}{\partial \delta_N} & \frac{\partial P_2}{\partial V_2} & \cdots & \frac{\partial P_2}{\partial V_N} \\ \vdots & & & \vdots & & \\ \frac{\partial P_N}{\partial \delta_2} & \cdots & \frac{\partial P_N}{\partial \delta_N} & \frac{\partial P_N}{\partial V_2} & \cdots & \frac{\partial P_N}{\partial V_N} \\ \hline \frac{\partial Q_2}{\partial \delta_2} & \cdots & \frac{\partial Q_2}{\partial \delta_N} & \frac{\partial Q_2}{\partial V_2} & \cdots & \frac{\partial Q_2}{\partial V_N} \\ \vdots & & & \vdots & & \\ \frac{\partial Q_N}{\partial \delta_2} & \cdots & \frac{\partial Q_N}{\partial \delta_N} & \frac{\partial Q_N}{\partial V_2} & \cdots & \frac{\partial Q_N}{\partial V_N} \end{array}\right] \tag{2.3}$$

The first row ($J_{P\delta}$ and J_{PV}) is partial derivatives of P with respect to δ and V, while the second row ($J_{Q\delta}$ and J_{QV}) is partial derivatives of Q with respect to δ and V. The Jacobian matrix is used to find the load flow solutions [45].

Reactive Power Compensation Calculations

To analyze how much active or reactive power is needed to correct voltage drops in the electricity grid, a voltage sensitivity approach can be used. The sensitivity matrix is extracted from the Jacobian matrix [48].

The sensitivity matrix is obtained from the inverse of the Jacobian matrix, as presented in Equation 2.4.1

$$\begin{bmatrix} \Delta\delta \\ \Delta V \end{bmatrix} = J^{-1} \begin{bmatrix} \Delta P \\ \Delta Q \end{bmatrix} \tag{2.4}$$

When using this approach, it is important to understand the structure of the matrix. The Jacobian matrix reflect the topology of the network in terms of load- and generation buses, and clearly, the sensitivity matrix will share the same size as the Jacobian. Similar to the Jacobian, the sensitivity matrix consist of submatrices. Each element of the sensitivity matrix gives information about how much P or Q at each bus would affect the V and δ at each bus. This is valuable information when calculating reactive power support, as it takes the whole grid topology into account. The sensitivity matrix takes the following structure, and the following submatrices:

$$S = \begin{bmatrix} S_{\delta P} & S_{\delta Q} \\ S_{VP} & S_{VQ} \end{bmatrix} = \left[\begin{array}{ccc|ccc} \frac{\partial \delta_2}{\partial P_2} & \cdots & \frac{\partial \delta_N}{\partial P_2} & \frac{\partial \delta_2}{\partial Q_2} & \cdots & \frac{\partial \delta_N}{\partial Q_2} \\ \vdots & & \vdots & \vdots & & \vdots \\ \frac{\partial \delta_2}{\partial P_N} & \cdots & \frac{\partial \delta_N}{\partial P_N} & \frac{\partial \delta_2}{\partial Q_N} & \cdots & \frac{\partial \delta_N}{\partial Q_N} \\ \hline \frac{\partial V_2}{\partial P_2} & \cdots & \frac{\partial V_N}{\partial P_2} & \frac{\partial V_2}{\partial Q_2} & \cdots & \frac{\partial V_N}{\partial Q_2} \\ \vdots & & \vdots & \vdots & & \vdots \\ \frac{\partial V_2}{\partial P_N} & \cdots & \frac{\partial V_N}{\partial P_N} & \frac{\partial V_2}{\partial Q_N} & \cdots & \frac{\partial V_N}{\partial Q_N} \end{array}\right] \tag{2.5}$$

Voltage sensitivity to reactive power, especially when it comes to controlling distributed generation, has been an explored topic of research [49]. proposes a particle swarm optimization algorithm and sensitivity matrix, where the main objective is to keep the voltage within specific limits and minimize the reactive power changes of distributed generation units [50]. uses the sensitivity matrix in an optimal power flow algorithm. The algorithm minimizes system operation costs, accounting for curtailment, energy losses, and the cost of reactive power.

Model predictive control of voltages is an approach used in multiple papers [51, 52]. A control scheme based on MPC using sensitivity indexes has been investigated in [51], where the controller was able to regulate the voltages during extreme operating conditions. [52] uses three layers of controls in a control scheme for active and reactive power, where MPC and optimal power flow are used. The concept of MPC will be elaborated in the next section about control theory.

The methodology for controlling the voltage with reactive power is also extensively researched. However, the drawback of the classical sensitivity matrix approach, is that the sensitivity coefficients are not constant and change according to the network operating point [49]. In addition, the relationship is also linearized around the operating point, which entails that there could be difficulties when the voltage deviation is too high. However, with the assumption that the variations in scheduled power prediction are as low as possible, using this strategy can be seen as reasonable [50].

2.4.2 Control Theory

This section will present the concepts and literature for different control strategies, mainly focusing on the three which are adapted in this thesis: rule-based, optimization using MILP and MPC control. A standard optimization problem is formulated in the following manner:

$$\min_{x} \quad f_0(x) \tag{2.6a}$$

$$\text{subject to} \quad f_i(x) \leq 0, \quad i = 1,...,m \tag{2.6b}$$

$$h_i(x) = 0. \quad i = 1,...,p \tag{2.6c}$$

The objective value (2.6a) is minimized, subject to a set of constraints. The constraints can be inequality constraints (2.6b) or equality constraints (2.6c). If both the objective function and constraints are linear, it is referred to as a linear programming problem. If one or more of the inequality constraints must take integer values, and some does not, it is referred to as a mixed-integer linear programming problem. This could if there was a combination on non-integer values and binary values. The vector x is referred to as the decision variables, and they can be varied within the bounds of the constraints, and together determine the value of the objective function. MPC is a control strategy that has gained a lot of traction in power system operation, as it can lead to increased accuracy in the control, given adequate predictions. A general MPC-control problem can be formulated as below:

$$\min_{u(k)} \quad \sum_{k=1}^{N} J\Big(x(k), u(k), d(k)\Big) \tag{2.7a}$$

$$\text{subject to} \quad x(k+1) = f\Big(x(k), u(k), d(k)\Big), \tag{2.7b}$$

$$\underline{x}(k) \leq x(k) \leq \overline{x}(k), \tag{2.7c}$$

$$\underline{u}(k) \leq u(k) \leq \overline{u}(k). \tag{2.7d}$$

The concept of an MPC algorithm is optimizing for a control horizon, execute the first control action, and create new predictions for the prediction horizon, before the process is repeated. J is the control objective, and f is the dynamic model of the system. x, u and d are the states, control inputs and disturbances [10]. The main drawback of this approach and other predictive approaches is that the computational effort and complexity are significantly higher than other control strategies. The need for good prediction algorithms is also a barrier in many cases [53]. Another approach is the rule-based programming approach. Rule-based programming is using formal logic as predefined rules in a program. The advantage of this method, it that it avoids the need for good forecasting for optimal operation and the complexity and computational effort can be lower than other methods [54]. In addition, another advantage of rule-based control is that is it relatively easy to understand and implement, compared to other more advanced strategies.

Optimal operation in power systems

There are different approaches to optimize energy management of the power system, which have distinct objectives which affect the overall performance of the power system. It can be technical in terms of minimizing voltage deviations, minimize reactive power transmission and minimize losses. It can also be directly economic, where the generators in the systems are dispatched to minimize the cost of generation and losses [45].

Table 2.4.2: An overview of the literature concerning energy management systems. The literature is highlighted in terms of optimization strategy, objective and main findings and the thesis is put in the same context for comparison.

Ref.	Summary	Model	Objective	Main findings
[55]	Battery scheduling algorithm for residential costumers of solar energy	LP	Min cost	The key factors affecting the viability of optimization are the tariffs and the PV/Load ratio at each inverter
[44]	Decision support tool for investment, optimal sizing and operation scheduling grid-connected PV/battery system	MILP	Max NPV	The model is capable of identifying the feasibility of an investment in PV and/or battery systems, and the specifications of the optimal system.
[56]	Optimization-based algorithm for the scheduling of residential battery storage co-located with solar PV, in the context of PV incentives such as feed-in tariffs.	QP	Max savings	The scheduling algorithm significantly penalizes reverse power flow and peak loads corresponding to peak time-of-use billing.
[57]	A predictive approach to control operation for an islanded microgrid with PV and wind production, battery, and H_2 storage at Rye, Trøndelag.	MPC	Min energy from diesel generator	The energy supplied by a diesel generator was reduced by 48.71 % compared to an existing model.
[58]	A hybrid MPC for smart charging with consideration of a buffer storage.	Hybrid MPC	Min grid power (et al)	The results successfully meet both system constraints and user convenience, whilst increasing the efficiency of charging.
[59]	Case study with different load profiles, utilizing EVs to balance demand	Rule-based	Min grid power	The renewable resource available and the EV could supply enough energy to the users demand in all seasons of the year.
[60]	Presents an EMS capable of forecasting PV production and optimized power flows between PV, grid, and EVs at the workplace	MILP	Min charging cost	The EMS provided a significant reduction in charging cost and increased profit.
[61]	A strategy for energy management of a microgrid with PV-battery systems and EVs	Rule-based	Max self-consumption	The proposed strategy was verified through experimental simulations and proved to be efficient for similar systems.

[62]	Strategy for real-time energy management for the EV charging station, which is equipped with renewable generation and BESS	MILP	Max self-consumption	The power peak of the local grid is mitigated largely by 52.98 % and the charging cost is also reduced by 31.7 %
Thesis	Providing three control strategies for a system equipped with a fast charging station, battery and PV system, including reactive power control	Rule-based, MILP and MPC	Min energy costs, min voltage impact	The combination of battery- and reactive power control was able to simultaneously minimize costs and limit grid impact. The MILP gave the lowest costs.

In [63], two rule-based strategies were proposed for storage operation, minimizing payments to the grid. The two strategies were able to achieve near-optimal performance without requiring forecasts. In [18], the results from the MILP optimization-based control strategy were more optimal than the rule-based approach. However, the trade-off between computational burden and optimality needs to be considered.

Combining a battery with PV is proven economically and technically feasible in [44, 55–62], given a good control strategy. As verified in [59, 61] a rule based control of the system is effective. However, other control methods are also studied and proved effective, such as the MILP approach [44, 60, 62]. As mentioned in the previous chapter, the MPC strategy of reactive power control is commonly used, and verified in various use cases [51, 52]. These three control strategies will be explored in detail in this thesis.

Chapter 3

System Description

As mentioned in the introduction, three battery controllers and a reactive power controller will be designed and validated by simulations in a grid model of the Stange distribution grid. This chapter describes the system used for these simulations. This includes a description of the Stange distribution grid and base load, power prices, and the system topology. There are also dedicated sections that describe each of the relevant components: The charging station, PV system, and stationary battery.

3.1 System and Grid Topology

Figure 3.1 presents the configuration of the controlled system. There is a transformer connected to the main distribution grid to step down the voltage. The power flow from the battery, PV system, and FCS power is converted from AC grid power to DC power through individual converters. A more detailed description of the components and their corresponding converters and inverters is presented in the next sections.

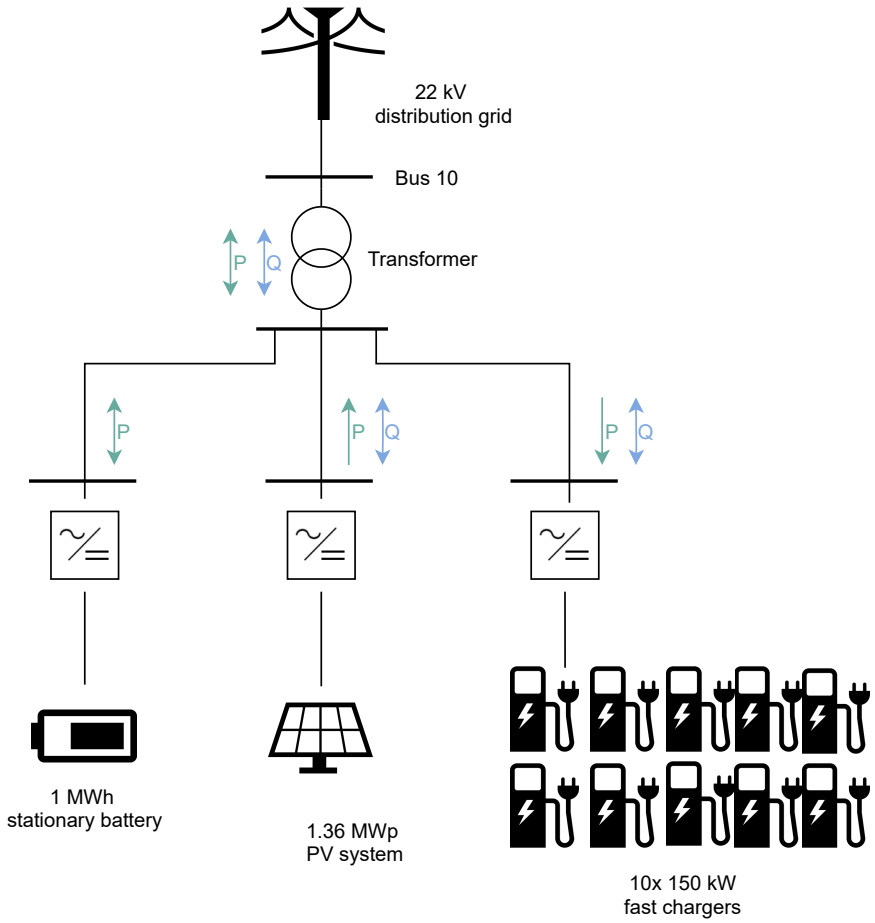

Figure 3.1: The system topology

Stange distribution grid, a 22 kV radial distribution grid located in Innlandet, is used to test the proposed control system. It consists of 11 buses, where 7 of the buses are connected to some time-varying load. The load at these 7 buses is referred to as the base load. The FCS and the associated components as presented in Figure 3.1 are simulated at bus 10. A single line schematic of the distribution grid is presented in Figure 3.2. Bus 1 is connected to a 22/66kV substation. It is underlined that the FCS, PV system, and stationary battery is just modeled and are not physically present in the distribution grid. The distribution grid is used for simulation purposes to verify the control strategies.

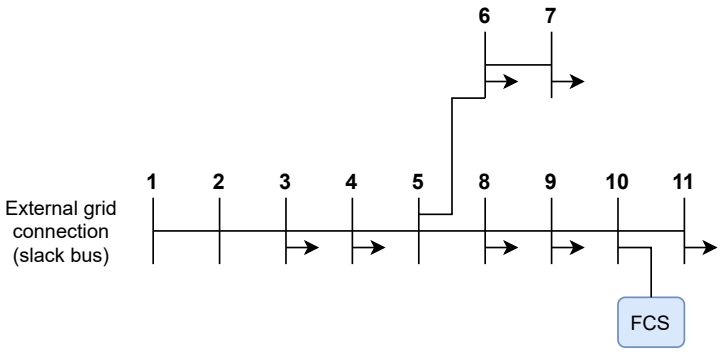

Figure 3.2: Single line diagram of the simulated distribution system. It consists of 7 load buses connected to some time-varying load (base load), bus 10 is the FCS bus which is connected to the PV system and battery. Bus 1 is the slack bus. Bus 11 is the most critical in terms of voltage, as it is the bus furthest away from the slack bus.

Three main profiles are used in the simulations: Predicted base load profiles, FCS load profiles, and PV production profiles. The base load of the distribution system is modeled based on SINTEF Energy Research general demand profiles for different customer groups [64]. It is distinguished between households and commercial buildings, and examples of customer groups are offices, agriculture, schools, and so on. The customer groups help to determine the load at the bus it is connected to. For a more detailed description of how the base load profiles for the Stange distribution grid are estimated, the reader is referred to [65].

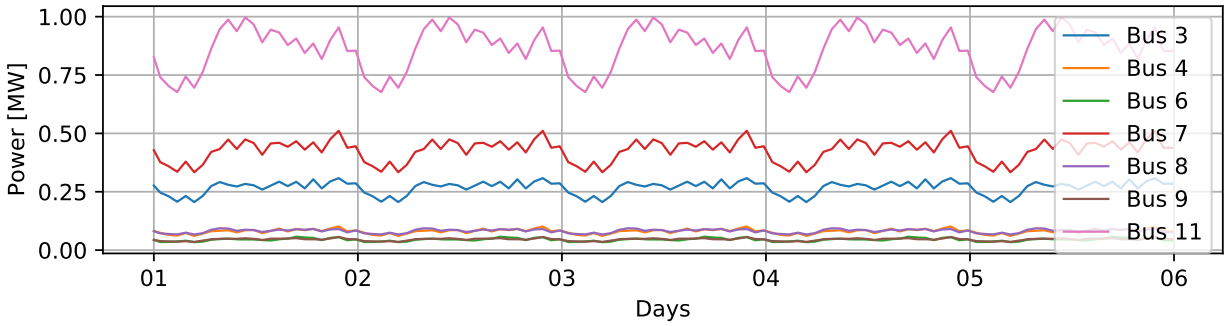

Figure 3.3: Daily load profiles for the base loads in the distribution system. There are base loads connected to buses 3, 4, 6, 7, 8, 9 and 11. The same daily load profiles are used as base load when multiple days are simulated.

As previously stated, this master thesis aims to find a control strategy for the FCS to limit the grid impact and minimize energy costs for the FCS operator. To get an interesting control problem, the FCS is simulated close to the critical bus, where the potential impact would be high.

When calculating prices, spot prices from 2019 are used, for a winter and summer situation. The prices from 2020 were significantly lower compared to previous years, and the 2019 prices were, therefore, the most recent year that was found more representative for a normal year. The prices are retrieved from Nord Pools historical market data [66]. The spot prices used are presented in Figure 3.4. The days are corresponding to the day of the year used for the PV power, to get a realistic seasonal picture. The winter days are 1st to 5th of January, and the summer days are 5th to 10th of July.

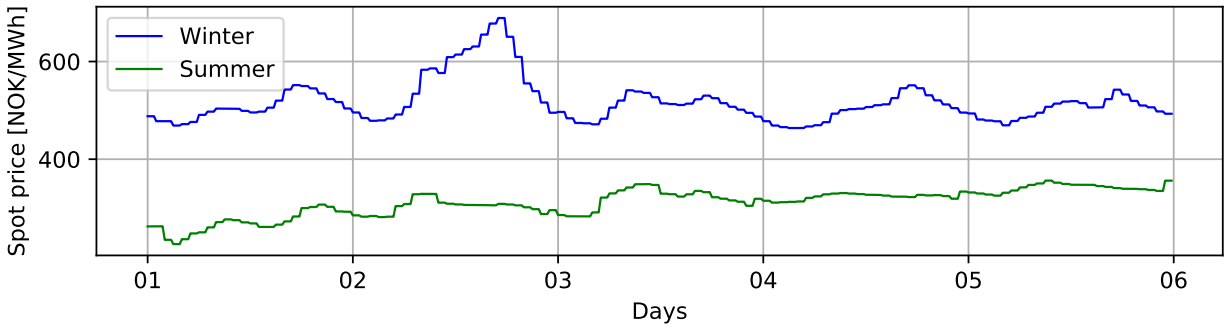

Figure 3.4: Five days of spot prices for summer and winter. Prices are historical market data from Nord Pool from 2019. The winter days are 1st to 5th of January, and the summer days are 5th to 10th of July [66].

3.2 Fast Charging Station

The fast charging station consists of 10 chargers with a maximum charging power of 150 kW. In this thesis, the aggregated load of the 10 chargers is considered. The maximum charging power from this FCS is therefore 1.5 MW. The size and number of chargers are based on the normal amount of chargers, and how the fast chargers will increase in rated power in the close future. On this basis, a combination of 10 charging outlets with a 150 kW rating was found fitting. The associated inverter has an aggregated rating of 1.5 MW, which is decided based on the FCS rating. As seen from Figure 3.1, there is an active and reactive power flow to the charging points. The active power flow to the fast chargers in a single direction, from either the battery, PV system, or grid. The FCS converter is also able to both inject and absorb reactive power as a response to the grid condition.

The program from [65] was used to obtain the load used as input for the simulation. The program uses stochastic load modeling and Monte Carlo Method to estimate the load at the FCS. A mobility model, a charging model, and a queuing model are used to simulate the system, and generating daily load profiles. Respectively, these models are used to determine the EV traffic flow, determine the load demand of the arriving EVs, and consider congestion at the FCS.

The MC simulation takes both deterministic and stochastic input. The deterministic input was the EV percentage, the number of charging points at the FCS, each charging point's rated power, EV fleet representation, and the maximum number of Monte Carlo simulations. Further, the stochastic input was the traffic flow and temperature profile generated for each iteration. A day was simulated for each iteration, generate arrivals, EVs, temperature dependencies, charging, and queuing model. The arrival of EVs was found from the percentage of EVs on the road in the area multiplied by the traffic flow. A realistic load profile for the charging points was obtained for each minute of a day. The resulting load profile is presented in Figure 3.5.

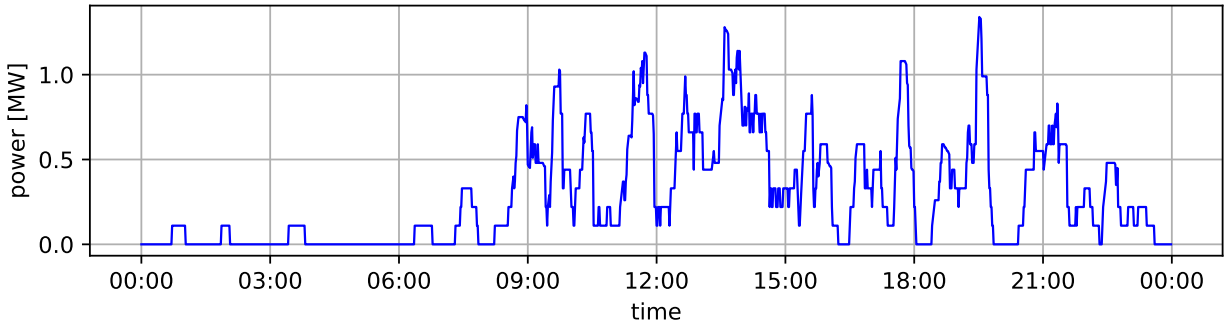

Figure 3.5: Daily load profile, for a single day with minute resolution. It is based on the stochastic load modelling method presented in [67].

To simulate multiple days at a time and relieve some of the computational efforts, the data was converted to 15-minute data. The resulting load profile for five days is presented in Figure 3.6.

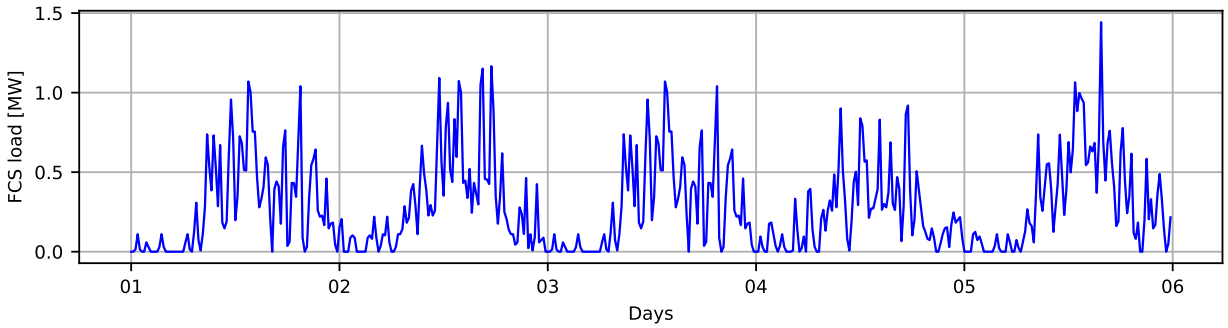

Figure 3.6: Daily load profiles, for five days with 15 minute resolution. They are based on the stochastic load modelling method presented in [67].

It is underlined that the load data is for random days. The days is not corresponding with the day or year of solar production and spot prices. Hence, the values used are estimated and not real values, but it is used to verify the model under different load and production conditions.

3.3 Photovoltaic System

The PV system used in the simulations is a 1.38 MWp system. The PV system's production is obtained from previous work done in [68], where data was acquired from simulating the PV system in PVsyst. The relevant parameters, e.g. solar irradiance data, were used from a weather station at Værnes. The modules used for the simulation in PVsyst were a combination of REC310 and REC295 Wp, yielding a total power of 86.4 kWp. The PV production is simulated for each hour of an entire year. This PV system and its yearly production are multiplied by a factor of 15 in this master thesis. Factor 15 is chosen because the size of the FCS in terms of nominal power is 15 times the FCS used in [18]. Therefore, the load and the production are multiplied by the same factor. There is no optimization behind the sizing of the components.

The inverter size is based on the DC-rating of the PV system, which is 1.38 MW. As seen from Figure 3.1, there is a unidirectional flow of active power from the PV inverter, which can either charge the battery or supply the load. The reactive power can either be absorbed or injected from the inverter. It is used two different PV production profiles to see how the system behaves in the extremes of the operation. The PV profiles are presented in Figure 3.7. The winter days are 1st to 5th of January, and the summer days are 5th to 10th of July.

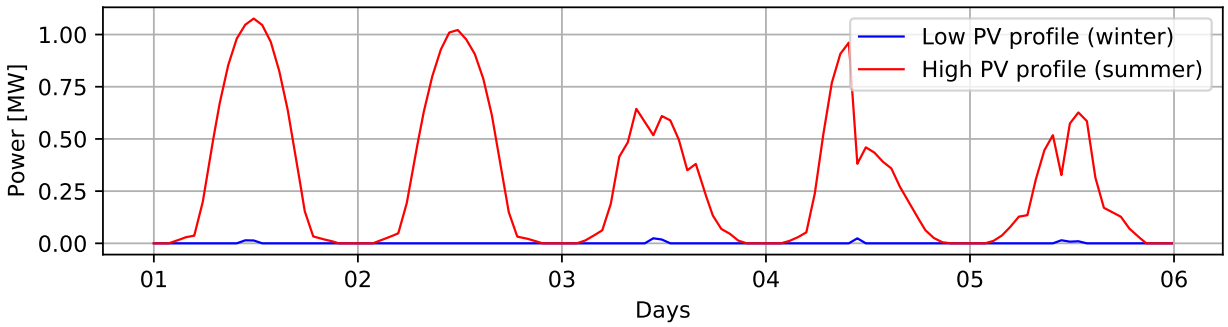

Figure 3.7: Two productions profiles. The winter days are 1st to 5th of January, and the summer days are 5th to 10th of July.

3.4 Stationary Battery

The stationary battery is modeled as a storage unit with a predefined capacity, maximum charging rate, and SOC limits. The specifications of the battery model are presented in Table 3.1. There is an upper and lower bound to the SOC because fully charging or discharging the battery could lead to an additional lifetime reduction. The maximum charging rate is chosen to be the same as the capacity, for simplification.

Table 3.1: Specifications of the stationary battery model.

Specification	**Battery**
Capacity	1 MWh
Maximum charging/discharging rate	1 MW
Lower SOC limit	20 %
Upper SOC limit	90 %
Charging/discharging efficiency	97 %

The size of the battery is decided by testing various capacities with the control structures and choosing the smallest capacity which gives an interesting control problem. This means that the battery is large enough to make an impact on the system, however, it is not so large that the battery is responsible for the voltage support alone.

The size is also considered in an economical matter, where the smallest possible capacity is chosen to minimize investment costs. It is underlined that other than the size aspect, the analysis of the battery is done in terms of economic operation rather than cost-benefit analysis, as optimal sizing is not within the scope of the thesis. There is no predictive data included in the model. However, realistic production and load data, as presented in the chapters above, is used to verify the model. How the battery is scheduled is described in detail in section 4.

Chapter 4

Methodology

This chapter gives a detailed description of the methodology in this thesis. An overview of the methodology step-by-step is presented in Figure 4.1. The load- and production modeling is done in previous work, however, the rest of the steps are all presented in this chapter. This includes grid modeling in pandapower, a description of the various control algorithms, and associated optimization problem formulations. A practical description of how the designed controllers are combined and implemented in pandapower is given. The designed controllers will be tested with the system model described in the previous chapter under different operational scenarios. Therefore, a description of how the simulation scenarios are organized is given. The chapter concludes with a summary of the methodology assumptions and limitations.

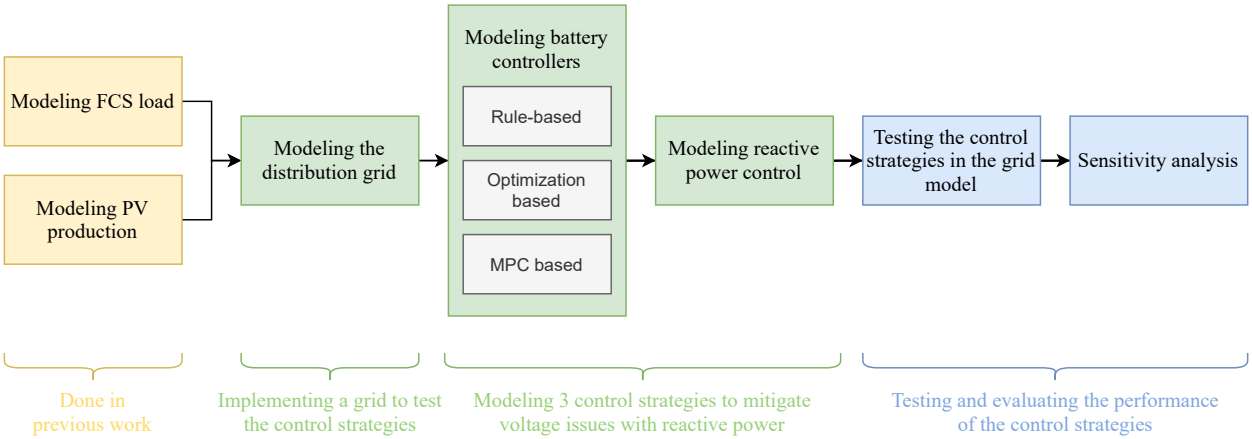

Figure 4.1: A summary of the methodology in the thesis work.

4.1 Grid Modeling

A grid model is necessary to analyze the impact of the FCS and various control strategies on the voltages in the distribution grid. This was done using an element-based python tool called pandapower. pandapower allows to run load flow analysis, and is aimed at the static analysis of balanced power systems [69]. This section will describe how the Stange distribution grid, as described in section 3, was modeled as a class in pandapower.

4.1.1 Distribution System Definition in pandapower

The grid model is built on an element basis. Examples of pandapower elements are buses, lines, loads, generators, and storage units. All elements are based on equivalent circuit models within the pandapower data structure, which are thoroughly validated against commercial software tools. The elements used to build a simplified grid model of the Stange distribution grid are buses, lines, loads, external grid connection, generator, and a storage unit. First, an empty network is defined, before all the elements are created. Starting with the buses, then the external grid, lines, loads, generation, and storage units.

The buses are the nodes of the network, and the buses are what connect all the lines, loads, generation, and storage elements. The nominal voltage has to be set for all the buses, and this is 22 kV for Stange. The lines of the network are the connection between the buses in the network and can be defined through a standard type library, or with custom parameters. The input parameters for lines are the network, connected buses, length, resistance, reactance, and capacitance per kilometer, and max thermal current. A more detailed description of the line parameters for Stange is given in [70]. The slack bus is modeled as an external grid connection in the power flow simulation, as it is connected to a higher-level power grid. The input parameters for the grid connection are the network and the bus where the slack is connected. In addition, the voltage magnitude per unit is defined as 1.

The loads in pandapower have a positive active power when it is consuming, and positive reactive power when it is absorbing. The required input parameters for defining a load are the network and which bus it is connected to. Other parameters might be defined as well, such as the active and reactive power of the load. A static generator has three required inputs: the network, bus to which it is connected, and active power of the generator. A storage unit is used when you have a time series simulation. As pandapower is not time-dependent, this has to be done manually. The required parameters for the storage unit are the network, connected bus, active power of the storage, and maximum energy capacity.

4.1.2 Time Series Simulation

To run a power flow simulation over a horizon, it is necessary to include a time series loop, which updates the powers for each time step. This is described in the flowchart in Figure 4.2. The time series loop is executed for each timestep and contains a control loop. The load flow is executed with a Newton Raphson algorithm.

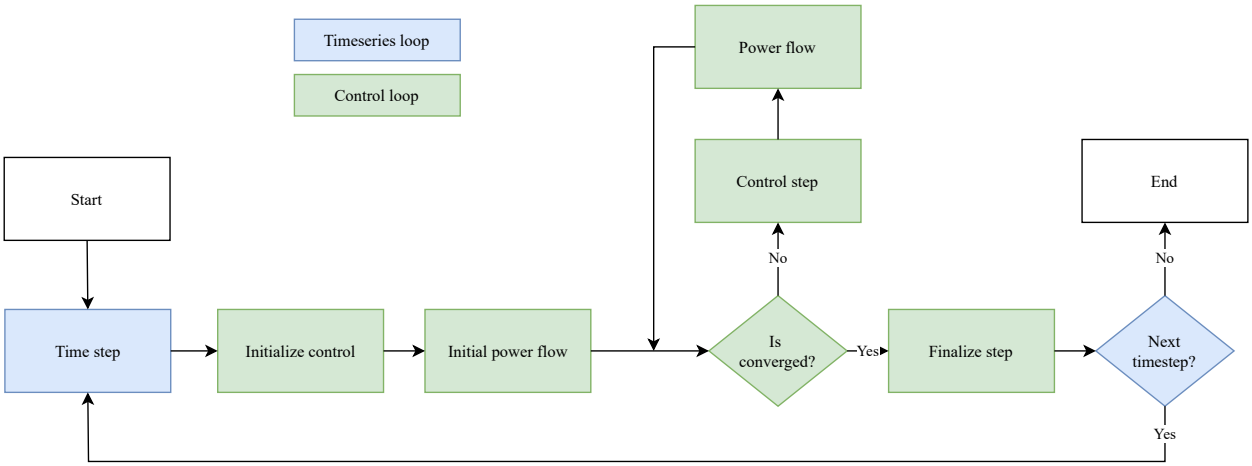

Figure 4.2: Time series module including a control loop [69].

4.2 Controller Modeling

This section presents the controllers developed in this thesis and their associated objectives. The control strategies are what control the active and reactive powers in the distribution system. Three different battery controllers are proposed. The rule-based- and optimization-based battery controllers have deterministic load and production values, which means that the power predictions used as a basis for the battery control are perfect and known. These two controllers are compared when it comes to operation. A third battery controller is also implemented, which takes into account errors in production- and load predictions, and this is the MPC-inspired battery controller. The MPC control is meant to demonstrate a way to deal with errors in production- and load predictions. As the predictions are imperfect, this approach is therefore referred to as having non-deterministic input. The MPC battery control is not directly compared to the others, as it is tested with different inputs and it would be an unfair comparison. In addition to the battery controllers, a reactive power control, both with and without battery present, is also designed and this is described in further detail.

4.2.1 Rule-Based Battery Controller

The rule-based battery controller is described in this section. It has the objective to minimize the grid imported power, in the sense that PV power is used for charging the battery, and the battery is not allowed to charge from the grid. Even though the main goal of the battery is to minimize energy costs, the controller does not take predictions for prices into account. Therefore, the goal is to try to achieve the same result by minimizing the energy imported from the grid.

First, the excess power is calculated, based on the load and production in that time step. This is the power that will either be used to charge/discharge the battery. If the excess power is positive, the battery will charge. First, an if-statement is used to check if the charging power will exceed the converter limit. If if it does, then the charging power is set to max and the rest is curtailed. If the limit is not exceeded, another if-statement is used to see if the charging at this rate will overfill the storage. If it will, then the maximum

power is used, and if it won't then the available power will be used. The same is done for discharging. The algorithm that is used for this control is presented in Figure 4.3.

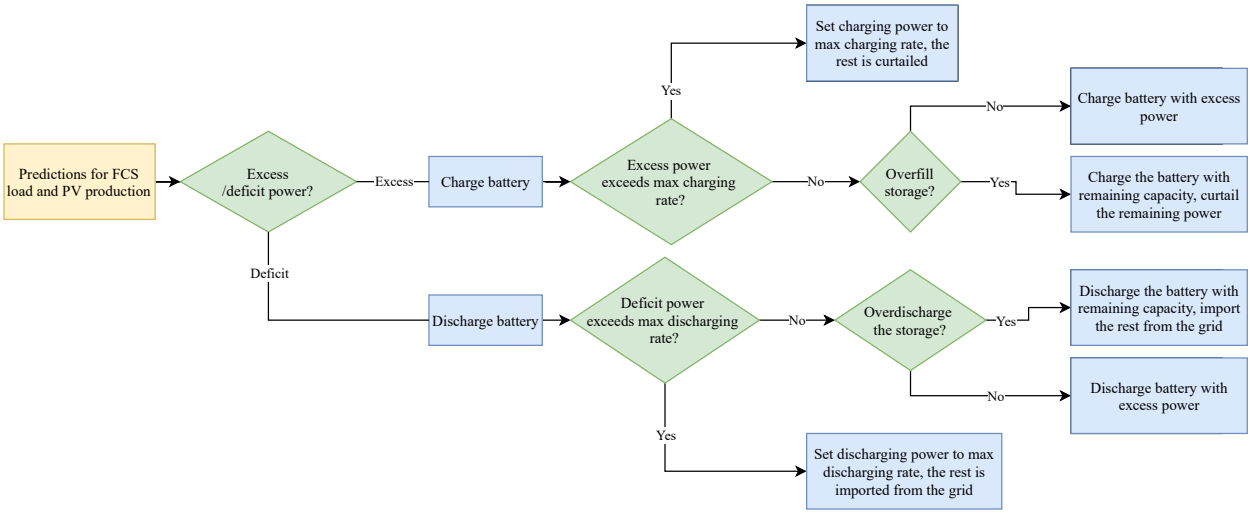

Figure 4.3: An overview of the rule-based battery controller algorithm. This is done for each timestep in the simulation, based on predictions for PV and load.

The resulting parameters from this algorithm is the battery charging power, updated SOC, and the curtailed power. The battery charging power is used in the next controller in the cascade, which is the reactive power controller, which is described in more detail in the next chapters.

4.2.2 Optimal Battery Controller

This section contains a description of the optimal battery control, which has a MILP problem formulation as described in subsection 2.4. The objective of this controller is to find a battery schedule that minimizes energy costs. The relevant objectives and constraints are presented in a generalized form below. The energy cost is the cost of electricity, which is the spot price multiplied with the power from the grid, no other price components, such as grid tariffs, are included. The load and PV balance constraints are that the load should always be met, and all the PV power should be distributed. The battery operation constraints are the charging and discharging of the battery, taking into account power bounds and efficiencies.

$$\min \quad \textit{energy costs} \tag{4.1a}$$

$$s.t. \quad \textit{load balance constraints,} \tag{4.1b}$$

$$\textit{PV balance constraints,} \tag{4.1c}$$

$$\textit{battery operation constraints,} \tag{4.1d}$$

$$\textit{variable bounds.} \tag{4.1e}$$

The algorithm minimizes the daily energy costs for the FCS operator. The optimization horizon is set to five

days for this controller, so the battery is scheduled for the following 5 days, assuming 100% deterministic values for load and production. The powers are optimized with a 15-minute interval, which is why the powers are divided by 4 when converted to MWh, such as in the objective function and SOC constraint. The optimization problem formulation, including objective and constraints, is presented below.

$$\min \quad \frac{1}{4}\sum_t \lambda_t \cdot \left(P_{GL,t} + P_{GB,t}\right) \tag{4.2a}$$

$$s.t. \quad P_{PL,t} + P_{BL,t}\delta_{D,t} + P_{GL,t} - P_{L,t} = 0 \tag{4.2b}$$

$$P_{PL,t} + P_{PB,t}\delta_{C,t} + P_{C,t} - P_{PV,t} = 0 \tag{4.2c}$$

$$\delta_{C,t} + \delta_{D,t} \leq 1,\ \delta_{C,t}, \delta_{D,t} \in [0,1] \tag{4.2d}$$

$$SOC_t = SOC_{t-1} + \frac{1}{4}\left[\eta_C P_{PB,t}\delta_{C,t} + \eta_C P_{GB,t}\delta_{C,t} - \frac{P_{BL,t}\delta_{D,t}}{\eta_D}\right] \tag{4.2e}$$

$$\underline{SOC} \leq SOC_t \leq \overline{SOC} \tag{4.2f}$$

$$P_{BL,t} \leq \overline{P}_B, \quad P_{PB,t} + P_{GB,t} \leq \overline{P}_B \tag{4.2g}$$

$$P_{PL,t},\ P_{BL,t},\ P_{GL,t},\ P_{PB,t},\ P_{GB,t},\ P_{C,t} \geq 0 \tag{4.2h}$$

Table 4.1: Description of the parameters and decision variables in the optimization problem.

Decision Variable	Description	Unit	Parameter	Description	Unit
$P_{PL,t}$	PV to load	[MW]	λ_t	Spot price	[NOK/MWh]
$P_{GL,t}$	Grid to load	[MW]	$P_{L,t}$	Load power	[MW]
$P_{BL,t}$	Battery to load	[MW]	$P_{PV,t}$	PV power	[MW]
$P_{PB,t}$	PV to battery	[MW]	$\overline{SOC}$	Upper SOC bound	[MWh]
$P_{GB,t}$	Grid to battery	[MW]	$\underline{SOC}$	Lower SOC bound	[MWh]
$\delta_{C,t}$	Charging binary variable	-	$\overline{P_B}$	Maximum charging power	[MW]
$\delta_{D,t}$	Discharging binary variable	-	ηC	Charging efficiency	%
SOC	State of charge	[MWh]	ηD	Discharging efficiency	%

The load should always be met, either by grid-, battery- or PV power, which is considered in Equation 4.2b. The generated power from the PV system has three possible destinations: the load, the battery, or it must be curtailed, which is formulated in Equation 4.2c. It should also be considered that the battery cannot be charged and discharged simultaneously. This is, therefore, considered by introducing two binary variables. Equation 4.2d makes it impossible to charge and discharge simultaneously. The updating of the SOC for each time step is considered in Equation 4.2e, and the bounds on the battery level are considered in Equation 4.2f. To not exceed the charging rate of the battery, Equation 4.2g is introduced. The power variables should all be positive, which is accounted for in Equation 4.2h. It can be observed that the variables are both integers (binary constraints) and non-integers (power values), and this is therefore a MILP problem. After

the optimization, the resulting battery charging power is used in the next controller in the cascade, which is the reactive power controller.

4.2.3 MPC-based Battery Controller

The last controller is the MPC-based controller. As mentioned, this controller is meant to demonstrate a way to deal with prediction errors, and this battery controller is not directly compared to the others, as it is tested on a different, non-deterministic input It uses the same objective and constraints as the optimal battery controller, however, the optimization horizon is a shifting horizon of 24 hours. This means for each timestep t, the predictions for load, production and prices are used as inputs for a 24-hour control horizon, and the powers are optimized from $[t, t+24]$. Based on the results, the first time step is applied, and then the process is repeated for the next timestep. This is repeated until the end of the simulation length, similar to MPC as described in section 2.

In reality, this battery schedule is sub-optimal, because the actual measured values will deviate from the predicted values to some extent. These deviations must be balanced somehow. Separate five-day load- and production profiles from the same production- and load models are used as predictions because creating a predictive algorithm is out of scope for this thesis. The profiles are presented in Figure 4.4 and Figure 4.5.

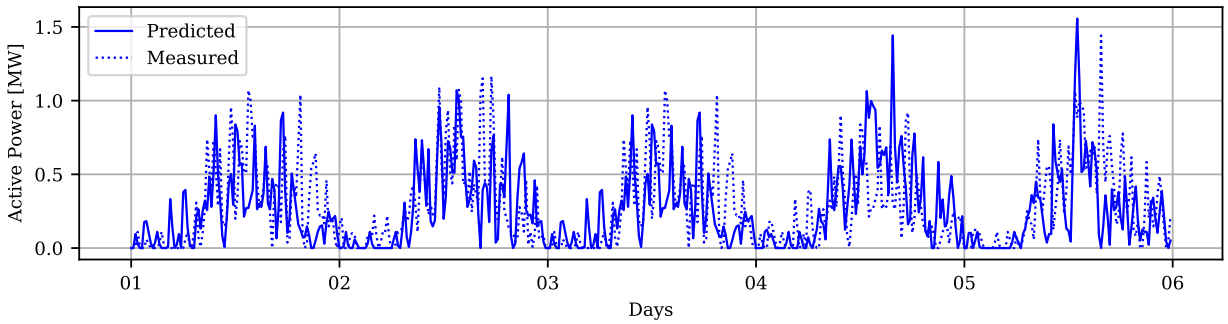

Figure 4.4: Predicted and measured load profiles used as input for the MPC based controller. The measured profile is equal to the load profile used to test the other control strategies.

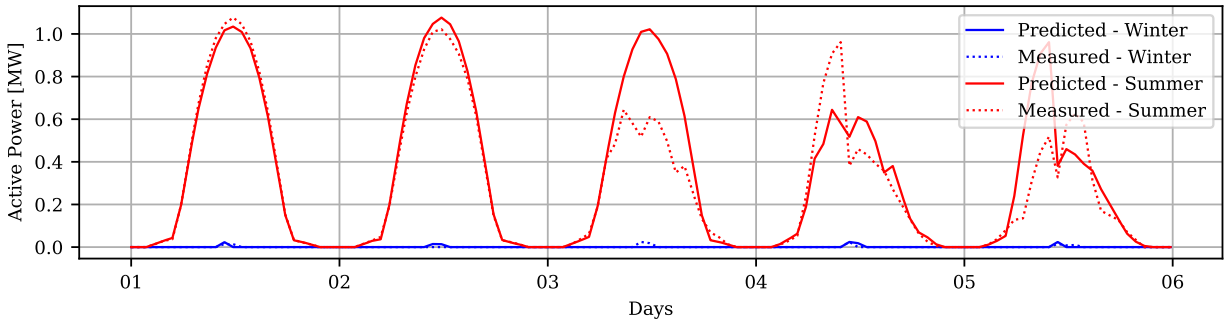

Figure 4.5: Predicted and measured PV production profiles used as input for the MPC based controller. The measured profiles are equal to the production profiles used to test the other control strategies.

The MPC-based control strategy first takes predictions for load and production and finds an optimal schedule for the next 24 hours. Further, the measured powers, according to the profiles above, are taken as input and the controller balances the powers based in a predefined order, which is illustrated in Figure 4.6. This rule-based power balancing is a quite simple way to balance the prediction errors.

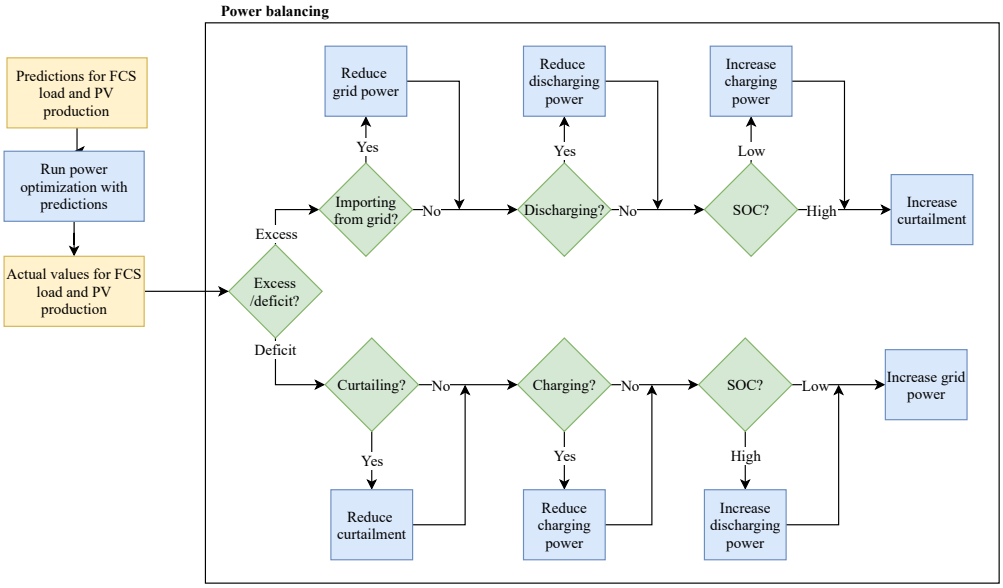

Figure 4.6: MPC-based control algorithm for the battery. The optimization is executed, before the errors are balanced like the flowchart illustrates. High and low SOC means that it is checking whether the charging power will overfill the storage, or not, and opposite for discharging.

When the powers are balanced, the next time step is initiated and the process is repeated for the next 24 hours, based on the new state of charge. In a more advanced MPC-control system, the predictions would change and hopefully improve, for each timestep. However, a single profile for predictions and measured values are used to demonstrate the power balancing, and what it would mean for the results. This limitation is further discussed in section 6.

4.2.4 Reactive Power Controller

The reactive power control algorithm takes the results from battery control as input and runs an initial load flow to see if this will exceed the voltage limits. If it does, then, the sensitivity matrix is calculated from the load flow result. As seen from Equation 2.4.1, the sub-matrix S_{VQ} provides the relationship between voltage difference and reactive power at the buses. The sensitivity sub-matrix S_{VQ} has the following structure:

$$S_{VQ} = \begin{bmatrix} \frac{\partial V_2}{\partial Q_2} & \frac{\partial V_2}{\partial Q_3} & \cdots & \frac{\partial V_2}{\partial Q_{10}} & \frac{\partial V_2}{\partial Q_{11}} \\ \frac{\partial V_3}{\partial Q_2} & \frac{\partial V_3}{\partial Q_3} & \cdots & \frac{\partial V_3}{\partial Q_{10}} & \frac{\partial V_3}{\partial Q_{11}} \\ \vdots & \vdots & & \vdots & \vdots \\ \frac{\partial V_{10}}{\partial Q_2} & \frac{\partial V_{10}}{\partial Q_3} & \cdots & \frac{\partial V_{10}}{\partial Q_{10}} & \frac{\partial V_{10}}{\partial Q_{11}} \\ \frac{\partial V_{11}}{\partial Q_2} & \frac{\partial V_{11}}{\partial Q_3} & \cdots & \frac{\partial \mathbf{V_{11}}}{\partial \mathbf{Q_{10}}} & \frac{\partial V_{11}}{\partial Q_{11}} \end{bmatrix} \tag{4.3}$$

The matrix component $\frac{\partial V_{11}}{\partial Q_{10}}$ tells us how much reactive power from bus 10 is needed to change the voltage at bus 11 a marginal amount. Multiplying this with the deviation from desired voltage will give the amount of reactive power that will correct the voltage to the desired voltage. ΔV is the difference between the desired voltage limit and the actual voltage.

$$\Delta Q_{10} = \frac{\partial Q_{10}}{\partial V_{11}} \cdot \Delta V_{11} \tag{4.4}$$

When the reactive power required from bus 10 is found, it is necessary to find out if there is sufficient capacity in the FCS or PV inverter to provide it. The active power of the PV and FCS is prioritized, which means that there is no load or production curtailment to supply reactive power. The reactive power available is calculated based on the converter/inverter ratings.

$$Q = \sqrt{S^2 - P^2} \tag{4.5}$$

If the required reactive power exceeds the available power, it is checked whether there is available capacity in the PV inverter. In other words, the reactive power from the FCS is prioritized, and if the capacity is not sufficient, the remaining will be supplied from the PV inverter. The available reactive power from the PV inverter is calculated in the same way as for the FCS, by using Equation 4.5. The resulting reactive power is assigned to the relevant controllers in the simulation, and this process is repeated for each timestep. If there is not sufficient reactive power capacity in both the PV inverter and FCS converter, then the voltage is only corrected with the available capacity. In other words, there is no backup voltage support if there is not sufficient reactive power available.

4.2.5 Controller Definition in pandapower

There are two main categories of controllers used in the program. The first is a *constant controller* which only has the job to update the powers. This is relevant for the fixed powers, such as the FCS load, PV power, and base load. The other type of controller is a *dependent controller*, which as the name implies, is used when the power is dependent on other powers or components. This is for example the battery controller, reactive power controller, and curtailed power controller. This type of controller includes calculations of the relevant powers in the python class before the load flow is executed.

A pandapower controller is modeled in an object-oriented framework. The controller object from pandapower contains four main methods, which are common for each controller. These are: is_converged, write_to_net, control_step and time_step. When running a time series simulation, the time_step method is the main action of the controller, and can be reading values from a profile, or doing calculations. What the time_step method contains depends on the controller type. The controllers used in the simulation in this thesis are presented in Table 4.2. The operations are what is included in the time_step method in the controller.

Table 4.2: Description of the modeled controllers in pandapower.

Controller	Element	Input	Operations	Output	Updating
Baseload	Load	Baseload profile	Update baseload powers	Base load power	Self
Charger	Load	FCS load profile	Update FCS power	FCS power	Self
PV	Generator	PV production profile	Update PV power	PV power	Self
RuleBased	Storage	FCS load profile, PV production profile	Rule based battery control algorithm	Grid power, curtailed power, updated SOC	Self, curtailment
OptBased	Storage	Optimal battery schedule	Update battery power and SOC	Grid power, Curtailed power, updated SOC	Self, curtailment
MPCbased	Storage	FCS load profile, PV production profile, spot prices	Run power optimization for a 24 h horizon. Generate errors. Balance powers.	Grid power, curtailed power, updated SOC	Self, curtailment
Reactive	Load	FCS load profile	Run load flow, and if the voltage exceeds limits, calculate reactive power	Reactive power	Self, PV
JointBattery-Reactive	Load	FCS load profile, PV profile, charging power, curtailed power	Run load flow, and if the voltage exceeds limits, calculate reactive power	Reactive power	Self
Curtailment	Storage	Curtailed power	Charge the curtailed power in a ”battery”	-	-

All of the mentioned controllers are used in the relevant control strategies. Which controllers are used in which control strategy is presented in Table 4.3. The base case with and without PV is not included in the three main control strategies. They are described in further detail in Table 4.4. The Reactive and JointBatteryReactive are in parenthesis because all of the control strategies can be run with and without reactive power control. This is done to analyze the impact of reactive power.

Table 4.3: Overview of which controllers in Table 4.2 that are used in the different control strategies in the thesis. The Reactive and JointBatteryReactive are in parenthesis because all of the control strategies can be run with and without reactive power control. This is done in order to analyse the impact of the reactive power.

Control strategy	Baseload	Charger	PV	Rule-Based	Opt-Based	MPC-based	Reactive	JointBattery-Reactive	Curtailment
Base case	✓	✓					(✓)		
Base case with PV	✓	✓	✓				(✓)		✓
Rule based	✓	✓	✓	✓				(✓)	✓
Optimization based	✓	✓	✓		✓			(✓)	✓
MPC based	✓	✓	✓			✓		(✓)	✓

4.3 Simulation Description

The simulations are carried out in five main parts: three scenarios a sensitivity analysis with deterministic inputs and one control strategy with non-deterministic inputs. The scenarios are the base case, low production case, and high production case. Each scenario will be presented with the battery operation (if relevant) and voltage control results. The structure of the results will be as presented in Figure 4.7.

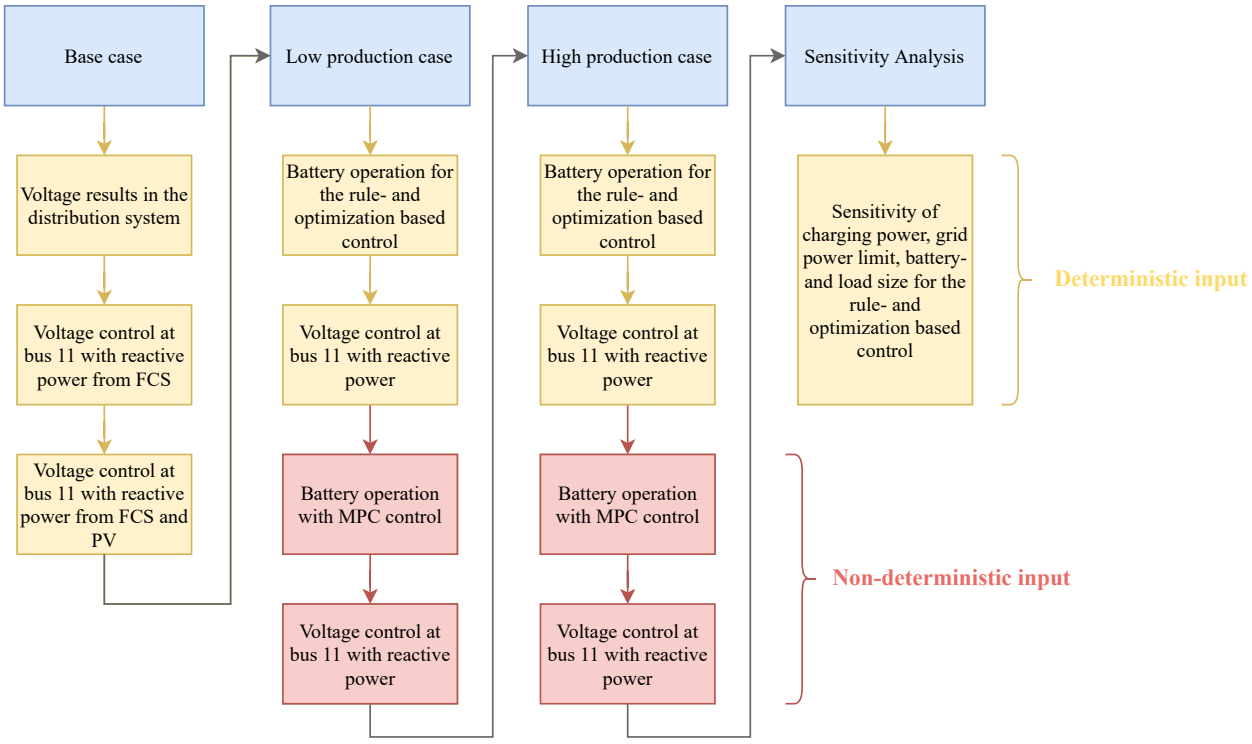

Figure 4.7: The structure of how the simulations are carried out.

The following paragraphs describe the three operational cases and the sensitivity analysis. All the cases are highlighted in terms of energy costs, reactive power usage, and system voltage. The two control strategies are compared: rule-based and optimal battery control, in combination with reactive power support. The description of each case is summarized below:

- **Base case:** The base case is meant to highlight how the system would behave if an FCS was implemented without battery or PV. This case is used as a basis for comparing to which degree the proposed control strategies will improve the system performance.
- **Low production case:** The low production case is meant to highlight how the system behaves when there is close to zero production. Is the system able to provide the given services, keeping the voltage within the limits? The purpose is to see which of the three control strategies is the most optimal under these conditions. The low production scenario in Figure 3.7 is used, which corresponds to 1st to 5th of January.
- **High production case:** The high production case is meant to highlight how the system behaves when

production is the highest throughout the year. Is the control system able to manage the system in a cost-efficient manner? The purpose is to see which of the three control strategies is the most optimal under these conditions. The highest production in Figure 3.7 is used, which corresponds to the 5th to 10th of July.

The base case is the scenario where there is no battery or PV system present, and it is what would happen if there were no additional components other than the FCS itself. In the low production scenario and high production scenario, there is both a PV system and battery present. The low production case has a high load and close to zero production throughout the day. The high production scenario has the highest daily production of the year and a high load. Each of the cases is run with the MPC-based control with non-deterministic inputs, which demonstrates a way to deal with prediction errors. Both the battery operation and voltage control are highlighted. Table 4.4 presents which components are present in the scenarios. The base case has PV in parenthesis because even though the PV production is not included, the impact of reactive power from the PV inverter is examined.

Table 4.4: Scenario description

Scenario	Base load	FCS load	PV	Battery
Base case	✓	✓	(✓)	
Low production case	✓	✓	✓	✓
High production case	✓	✓	✓	✓

A voltage of 0.95 pu is chosen as a lower limit when correcting the voltage drops. Even though the regulations indicate that the voltage drops can vary by $\pm 10\%$ of nominal voltage [71], a stricter correction is chosen. The voltages do not drop below 0.90 pu in the simulated system, and it would not be an interesting control problem if the limit was 0.90 pu. However, the control strategies can be transferred to other systems, and the voltage limit can be adjusted to fit the DSO needs.

The sensitivity analysis is conducted to highlight how a slight change in different variables would influence the operation. This is done to understand which variables impact the operation the most, and where there is room for improvement. It is conducted only for the low production case because the system must be able to meet the requirements even when there is limited local production. The reason for each of the sensitivity analysis is summarized below:

- **Upper limit on voltage:** In the simulated distribution grid, none of the buses inject active power to the grid. This means that no factors are causing the voltage to rise, other than reactive power injection at bus 10. However, in other systems, over-voltage might be an issue. Therefore, the control system is tested with an upper limit on the voltage.
- **Charging power limit:** The battery is programmed to optimize energy costs, and while this is beneficial for the charging station operator, using grid power to charge the battery might cause voltage issues. To address this, the maximum power that the battery can charge is adjusted, to see if this has a positive impact on the grid.
- **Grid power limit:** Because a significant part of the electricity bill for the FCS operator is the capacity

charge, which is decided by the peak power, it is relevant to use the battery for peak load reduction. It is therefore relevant to see the voltage impact of putting a maximum power limit for grid imported power.

- **Battery size:** This is done because there is no optimization behind the battery size used in the case analysis, and it is therefore interesting to see how a different size would have an impact, both when it comes to costs and reactive power usage.
- **Load size:** As the overall trend is towards higher charging powers, it is relevant to analyze how this system would behave with an increased power rating. How sensitive are the battery operation and voltage to the change in load? Is the system still able to stay within limits?

Some metrics are used to compare the sensitivity results to the original inputs. They are voltage within limits, average deviation from limit, injected reactive energy, and percentage change. A description of the metrics is given below.

Table 4.5: Descriptions, calculations and units for the outputs of the sensitivity analysis, which are the base for comparison.

Output	Description	Calculation	Unit
Voltage within limits	The percentage of time the voltage is within the limits.	For each timestep, it is checked whether or not the voltage limit is exceeded. If it is, this is added to the number of violations, and the total number of violations is divided by the number of timesteps	%
Average deviation	The average deviation from the voltage limit	If the voltage is exceeded, the deviation from the limit is calculated, and this is averaged over the total number of violations.	pu
Minimum voltage	The lowest voltage at bus 11 throughout the period	-	pu
Injected RE	Reactive energy (RE), the integral of reactive power injected over time.	$\frac{1}{4}\sum_{t=0}^{T} Q_t$	MVARh
Cost	The cost of importing power from the grid, only accounting for spot prices of electricity	$\sum_{t=0}^{T} \lambda_t \cdot (P_{GB,t} + P_{GL,t})$	NOK

These outputs are compared in the sensitivity analysis, based on the percentage change from the original output. The percentage change, which will be referred to as Δ, is calculated in the following way:

$$\Delta = \frac{\text{output(new input)} - \text{output(original input)}}{\text{output(original input)}} \tag{4.6}$$

4.4 Assumptions and Limitations

In reality, there would be a distribution transformer to meet the voltage of the FCS system. However, this transformer is assumed to have a low impact on the system behavior and is therefore omitted in the model. This is compensated for as an increased loss factor in the charging and discharging of the battery. The base load in the grid is also assumed to be the same for each day and is not dependent on the season. When it comes to the base load of the distribution grid, only the active power is considered. Hence, the injection or absorption of reactive power happens exclusively in buses 1 and 10. As previously mentioned, the size of the components is based on realistic sizes, however, they are decided on a heuristic basis.

A time step length of 15 minutes is used in the simulations. For the optimization-based control strategy, the optimization horizon is 5 days, and for the MPC-based control, the optimization horizon is 24 hours. Even though the load profiles are provided with 1-minute intervals, the data is converted to 15-minute data. This is to decrease the computational effort of the problem. The PV production data is provided in hourly data, and it is assumed a linear increase/decrease between each hour. The predictions for the base load are considered to be perfect. This is for all the simulations except when the MPC-based control strategy is used. The MPC predictions are assumed to be constant, and not updated for each time step. The FCS is assumed to pay for spot prices in the energy price calculations, and no additional grid tariffs are considered in the analysis. For simplicity, the PV system is not allowed to inject power back to the grid. It is only allowed to supply the FCS or the battery.

Chapter 5

Results

This chapter presents all the results related to the scenarios described in section 4. The results are presented for the base case, low production, and high production scenario. This includes an overview of the voltage control and reactive power management for the base case, and voltage- and battery control for the low- and high production case. The last section provides a sensitivity analysis, which is meant to highlight how the system acts with other inputs and to gain deeper insights into the results. The sensitivity analysis includes reduced charging power- and grid limit, increased/reduced battery size, and increased load.

5.1 Base case

The base case contains the load situation that would occur in a situation with an FCS at bus 10 if there were no additional components. It is meant to highlight how the system would behave if an FCS was implemented without battery or PV. The result on the voltages in the distribution system is presented in Figure 5.1. It can be seen from the figure that the voltage at buses 9, 10, and 11 drops below the limit of 0.95 pu at some instances. As mentioned previously, bus 11 is the bus furthest away from the slack bus. It is, therefore, the most critical in terms of voltage, which also can be observed from Figure 5.1. Bus 11 will therefore be the focus of the analysis. In this case, the voltage at bus 11 is above the limit of 0.95 pu 87.1% of the time, and the voltage drops to 0.932 pu at the worst.

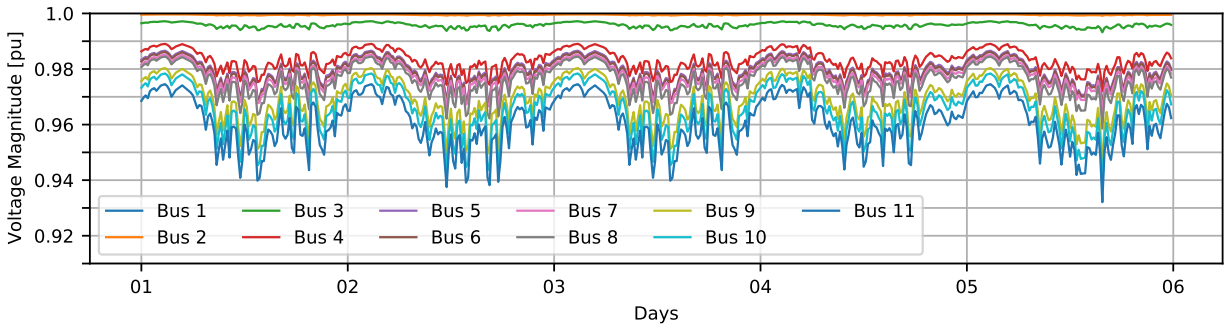

Figure 5.1: The voltage at the buses, with the baseload and FCS load. The voltage at bus 9, 10 and 11 drops below 0.95 at some point, and some sort of compensation is needed. The voltage is within limits 87.1% of the time and the lowest voltage is 0.932 pu.

5.1.1 Reactive Power Support

When introducing reactive power from the FCS as voltage support, the voltage is closer to the limit of 0.95 pu. This can be seen from Figure 5.2. The base load is the green line, which is the voltage without the FCS load. The dotted red line is the voltage with FCS load, and it can be seen from the blue line that the voltage is kept from dropping too far below 0.95, and the lowest voltage is increased from 0.932 to 0.935 pu.

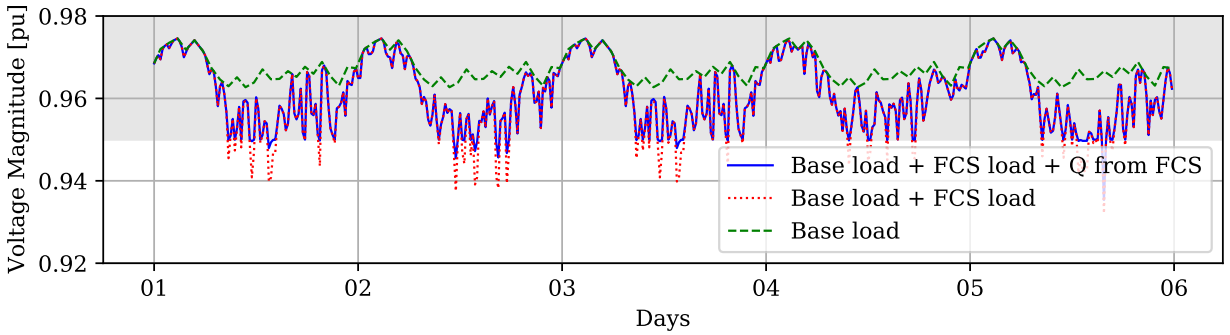

Figure 5.2: Voltage at bus 11, the most critical bus. This figure illustrates the impact of reactive power support on FCS and base load. When adding FCS load at bus 10, the voltage has many instances where it drops below 0.95. With reactive power support from the FCS, the voltage is kept approximately at 0.95 during critical times. However, there are still some violations.

Even though the deviation from the limit is reduced, there is still a voltage drop at 16:00 on day five. It can be seen from Figure 3.6 that at this specific hour, the load is almost at the rated power of the FCS, and therefore, close to zero reactive power capacity. Table 5.1 shows the difference in voltage characteristics and costs with and without reactive power. The reactive power from the FCS is sufficient most of the time. However, during the most critical hours, such as the afternoon on day five, there is a need for additional compensation. The effect of having increased reactive power capacity, by using a PV inverter, the results are as presented in the last column of Table 5.1.

Table 5.1: Voltage and cost results for the system with and without reactive power in the base case

Base case	**Without reactive power**	**With reactive power (FCS)**	**With reactive power (FCS+PV)**
Within voltage limits	87.9 %	97.7 %	98.3 %
Average deviation	$4.7 \cdot 10^{-3}$ pu	$0.66 \cdot 10^{-3}$ pu	$0.31 \cdot 10^{-3}$ pu
Minimum voltage	0.932 pu	0.935 pu	0.945 pu
Cost (winter prices)	18 438 NOK	18 438 NOK	18 438 NOK
Cost (summer prices)	10 936 NOK	10 936 NOK	10 936 NOK

It can be seen that this increased the minimum voltage close to the limit of 0.95 pu, and also reduces the deviation from the limit. The reactive power usage distributed between FCS and PV inverter is presented in Figure 5.3. Reactive power from additional components such as PV inverter, is desirable when the FCS load is close to peak, because the reactive power capacity is close to zero, and the associated voltage drop is high. It is therefore seen that the PV inverter can be used to correct the voltage drop in the afternoon on day five.

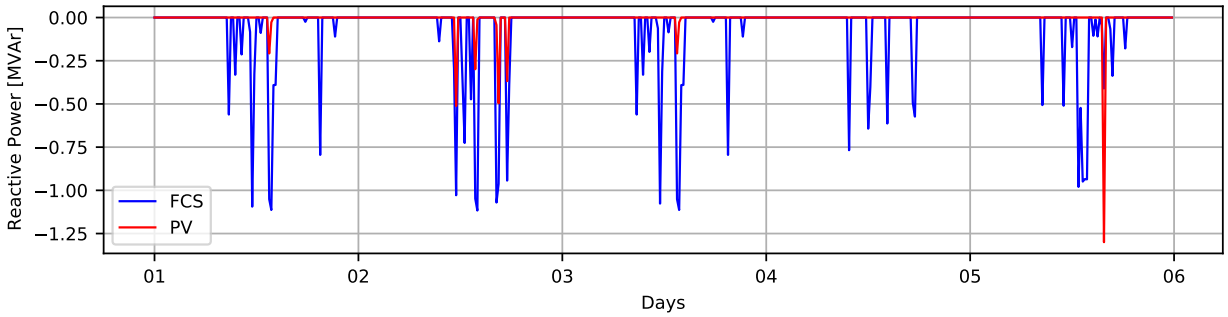

Figure 5.3: The amount of reactive power supplied from the PV inverter and FCS in the base case.

As reactive power has no direct market effect, the costs are the same with and without reactive power, as seen from Table 5.1. However, the voltage is improved both in terms of minimum voltage and average deviation from the limit, when using reactive power to compensate. When using only the FCS, there are still some instances where it is not sufficient, and additional components are necessary. Even though the voltage results are acceptable with only reactive power, there is still potential for energy cost reduction, as all of the power is supplied from the grid.

5.2 Low Production Scenario

The low production scenario contains close to zero production, as presented in Figure 3.7. This case is meant to highlight how the system behaves when there is close to zero production. This section will provide results for the battery operation and voltage control under these conditions. The voltage profile for bus 11 with the low production, without any battery, is presented in Figure 5.4. The voltage stays within an acceptable range 88.1% of the time, with a minimum voltage of 0.932 pu. The introduction of PV power does not have a significant impact in this case, as the production is close to zero. The battery, therefore, plays an important role in this scenario.

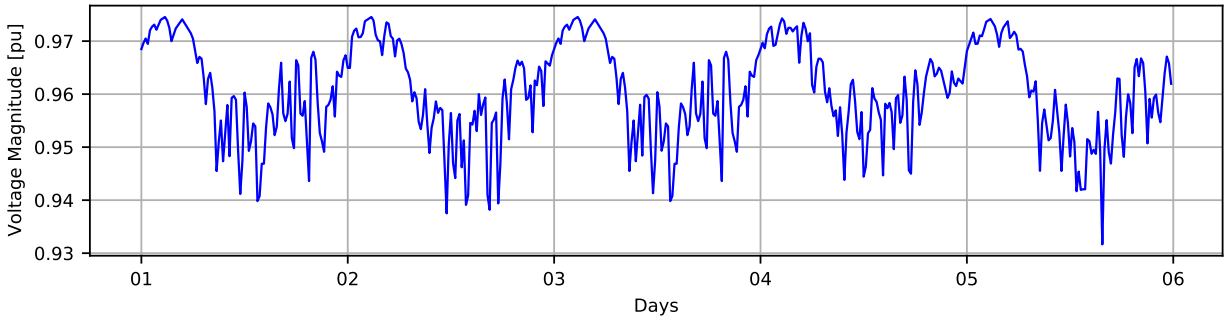

Figure 5.4: The voltage profile at bus 11 for the low production case if there was no battery. The voltage stays within an acceptable range 88.1% of the time in winter and the lowest voltage is 0.932 pu.

5.2.1 Battery operation

The results for the battery state of charge for the two control strategies are presented in Figure 5.5. In terms of battery utilization, the rule-based approach does not give very good results. Because this control strategy does not allow charging the battery from the grid, the battery is not able to recharge throughout the period and the battery capacity is not retained for a long time.

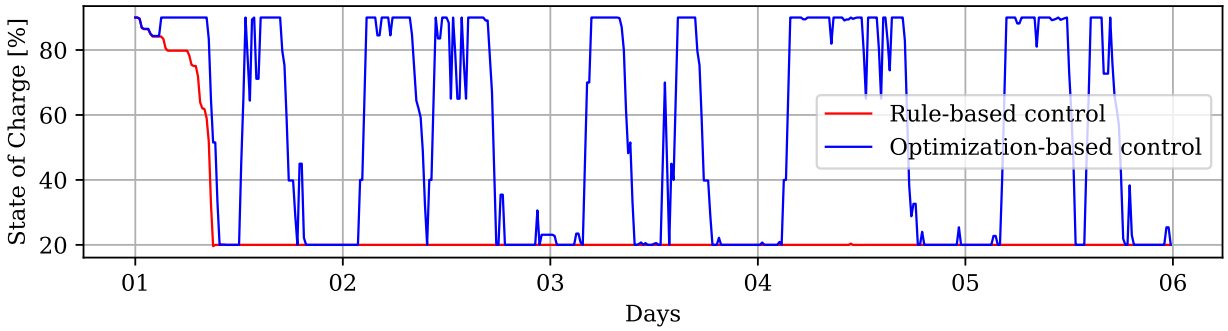

Figure 5.5: This figure shows the SOC of the battery with rule-based control and optimization based control for five consecutive days. The load and production profile is according to Figure 3.6 and Figure 3.7.

Figure 5.6 and Figure 5.7 illustrates the voltage impact of the battery for the rule-based control and optimization-based control. The voltage profiles show that using the battery for energy cost-optimization without grid

considerations has a significant impact on the voltage. The shaded area is the acceptable voltage bound.

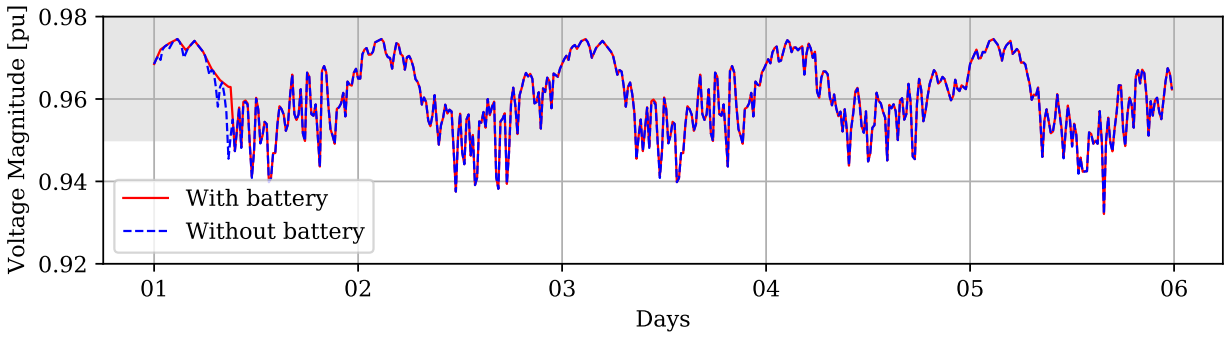

Figure 5.6: The voltage profile at bus 11 with and without battery with a **rule-based battery control**. The battery does not have a significant impact on the voltage profile, and the minimum voltage is still 0.932 pu.

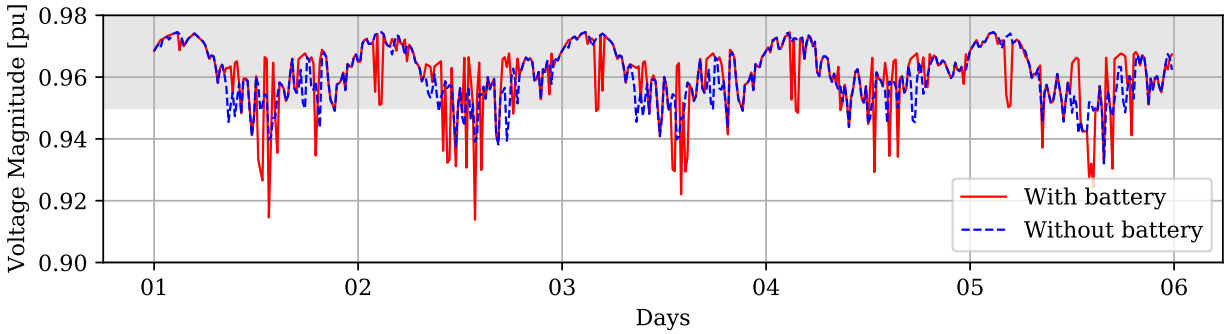

Figure 5.7: The voltage profile at bus 11 with and without battery with an **optimization based battery control**. The minimum voltage is 0.914 pu, which is a decrease compared to the base case.

The battery can charge from the grid in an optimization-based control strategy, and therefore, the PV and grid power can be utilized more strategically in terms of prices. It can be seen from Table 5.2 that the cost is lower with an optimization base control.

Table 5.2: Voltage and cost results for the two strategies with battery in the low production case.

Low production case	No battery	Rule-based	Optimization based
Within voltage limits	88.1 %	88.3 %	87.9 %
Average deviation	$4.7 \cdot 10^{-3}$ pu	$4.7 \cdot 10^{-3}$ pu	$10.9 \cdot 10^{-3}$ pu
Minimum voltage	0.932 pu	0.932 pu	0.914 pu
Cost [NOK]	18 375 NOK	18 035 NOK	17 650 NOK

5.2.2 Voltage Control with Reactive Power

The control of the battery is combined with reactive power control. As a reminder, the control of the battery happens first, minimizing cost, before the resulting power is used as a basis for calculating the required

reactive power. As it can be seen from Figure 5.6 and Figure 5.7, reactive power compensation is needed, because of the significant impact of the battery. The voltage results after the reactive power support is presented in Figure 5.8 and Figure 5.9. The system can stay within the voltage bounds to a larger extent with the rule-based approach. For the optimization-based control, there are significant voltage drops in the afternoon day 1 and 2. The combination of FCS and PV reactive power is not able to correct a voltage drop of this magnitude, and the minimum voltage is 0.931. This is slightly lower than the base case without reactive power.

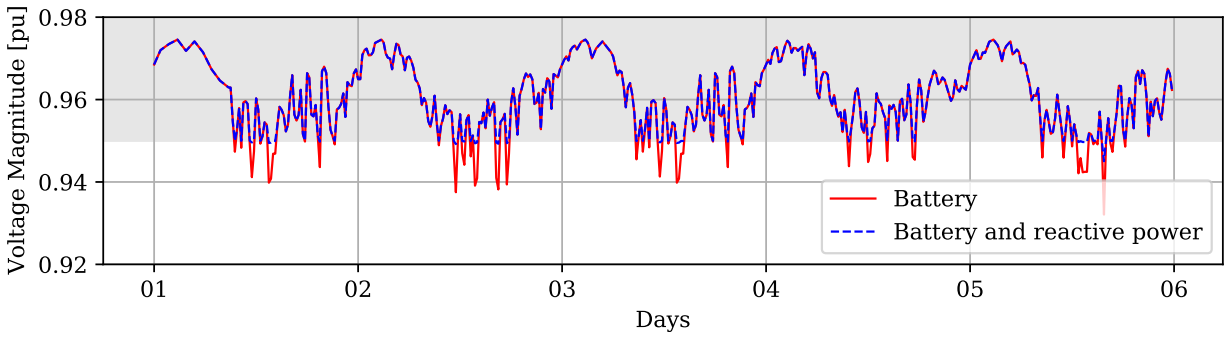

Figure 5.8: The voltage profile at bus 11 with and without reactive power support with the **rule-based battery control**. The minimum voltage is increased from 0.932 pu with battery to 0.945 pu with additional reactive power support.

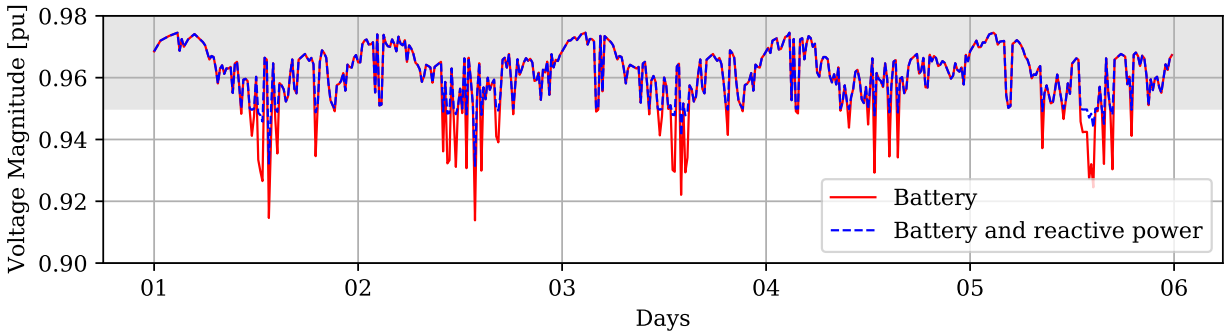

Figure 5.9: The voltage profile at bus 11 with and without reactive power support with the **optimization based battery control**. The minimum voltage is increased from 0.914 pu with battery to 0.931 pu with additional reactive power support.

Figure 5.10 shows the injected reactive power at bus 10 seen from the system point of view. This means that negative power indicates injection from the system to the grid. The reason why the rule-based result for Figure 5.10 is quite similar to Figure 5.3, is because the battery is empty for most of the time, and it is therefore quite similar to the base case. When it comes to the optimization-based control, it can be observed that there is a significantly higher amount of reactive power injected. This is because the battery caused higher voltage drops, as seen from Figure 5.7, and the demand for reactive power is much higher.

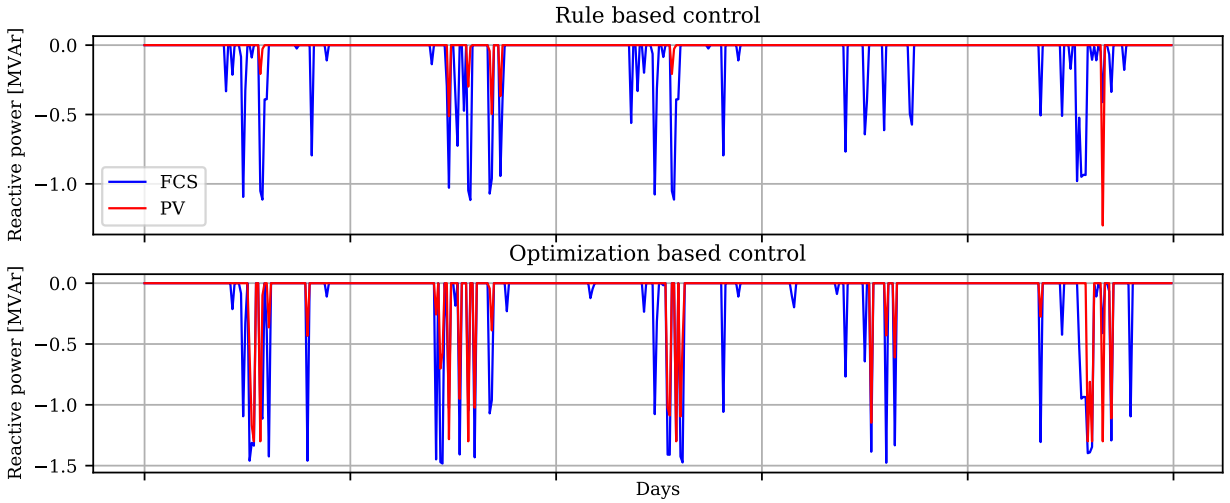

Figure 5.10: The amount of reactive power supplied from the PV inverter and FCS in the low production case with the two control strategies.

The voltage, reactive power and cost results are presented in Table 5.3. It can be seen that the amount of reactive energy required is increased substantially with the optimization-based control strategy. The main takeaway from this case is that with the given system, objectives, and price structure, there is a trade-off between energy costs and voltage limit violation. This could be addressed by having other objectives or tariff structures, which will be further discussed in section 6.

Table 5.3: Voltage and cost results for the two control strategies with reactive power and battery.

Low production case	**No battery**	**Rule-based**	**Optimization based**
Within voltage limits	98.5 %	98.5 %	94.0 %
Average deviation	$0.24 \cdot 10^{-3}$ pu	$0.24 \cdot 10^{-3}$ pu	$1.63 \cdot 10^{-3}$ pu
Minimum voltage	0.945 pu	0.945 pu	0.931 pu
Reactive energy injected	8.86 MVArh	8.72 MVArh	19.18 MVArh
Cost	18 375 NOK	18 035 NOK	17 650 NOK

5.2.3 With Prediction Errors

This section is meant to demonstrate the simple MPC-inspired control algorithm, taking into account the stochasticity of the load and production. Figure 4.4 and Figure 4.5 are the input for load and PV production in the algorithm, respectively. The winter profiles in Figure 4.5 are used as the low production scenario. As both the measured and predicted production is quite low, the load is the main contributor to prediction errors. To deal with the deviations, the balancing algorithm in section 4 is implemented, and the results for the SOC are presented in Figure 5.11. It can be observed that introducing prediction errors leads to sub-optimal performance. The optimal trajectory is what would happen if the inputs were deterministic, and therefore known beforehand and used to find the optimal schedule. The optimal SOC is therefore corresponding to the optimal battery control, as described in the previous section.

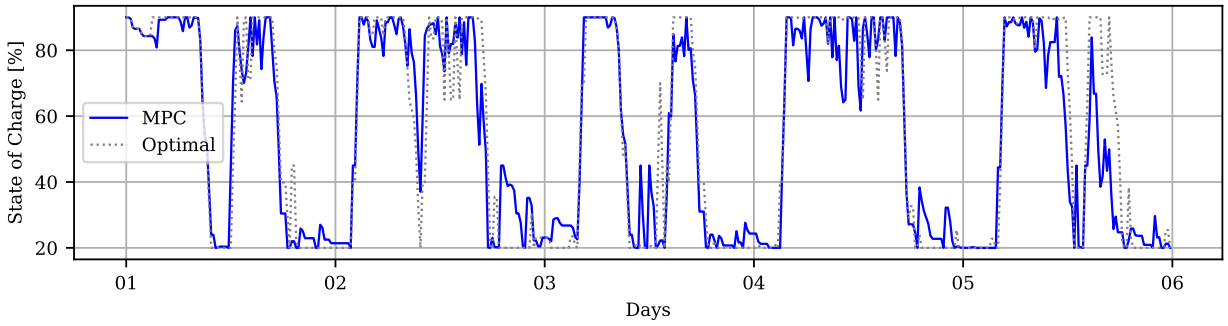

Figure 5.11: SOC of the battery during winter when there is low production. The optimization happens with a shifting 24-hour horizon.

Table 5.4 presents the voltage- and cost results for the MPC-based control, for low production, with and without reactive power support. There is a significant improvement when it comes to both average deviation and minimum voltage when reactive power is used as additional support.

Table 5.4: Voltage and cost results for the two control strategies.

MPC based	**Without reactive power**	**With reactive power**
Within voltage limits	85.2 %	94.8 %
Average deviation	$7.8 \cdot 10^{-3}$ pu	$0.74 \cdot 10^{-3}$ pu
Minimum voltage	0.921 pu	0.939 pu
Reactive energy injected	0 MVArh	17.7 MVArh
Cost	17 693 NOK	17 693 NOK

5.3 High Production Scenario

The high production scenario contains high load and high production, as presented in Figure 3.6 and Figure 3.7. This case is meant to highlight how the system behaves when production is the highest throughout the year. This section will provide results for the battery operation and voltage control under these conditions. The voltage profile for bus 11 with the high production case is presented in Figure 5.12. The voltage stays within an acceptable range 98.3% of the time, with a minimum voltage of 0.936 pu. This illustrates that the use of a PV system is decreasing the grid impact of the FCS load. Because the PV production is not controllable, the battery plays an important role in reducing the peak load in this scenario.

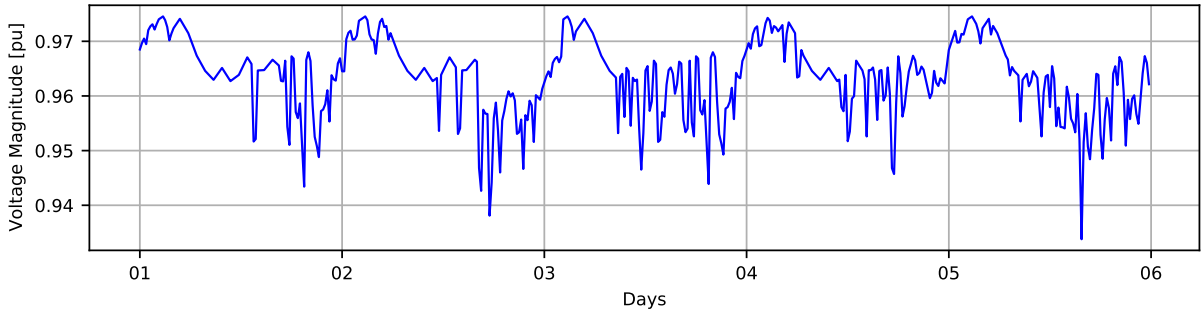

Figure 5.12: The voltage profile at bus 11 for the low production case if there was no battery. The voltage stays within an acceptable range 98.3% of the time in summer and the lowest voltage is 0.936.

5.3.1 Battery Operation

The results for the battery state of charge for the two control strategies are presented in Figure 5.13. Here, the SOC trajectories are more similar to each other than in the previous case. Even though the rule-based control does not allow charging the battery from the grid, the PV production is sufficient to recharge.

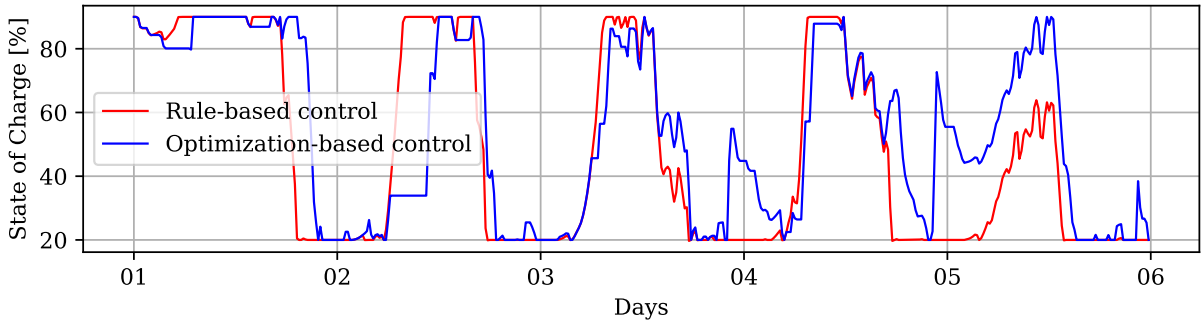

Figure 5.13: This figure shows the SOC of the battery with rule-based control and optimization based control for five consecutive days. The load and production profile is according to Figure 3.6 and Figure 3.7.

Figure 5.14 and Figure 5.15 illustrates the voltage impact of the battery for the rule-based- and optimization-based control respectively. The voltage profiles show that the battery and PV production can keep the voltage above limits to a larger extent, without any reactive power support.

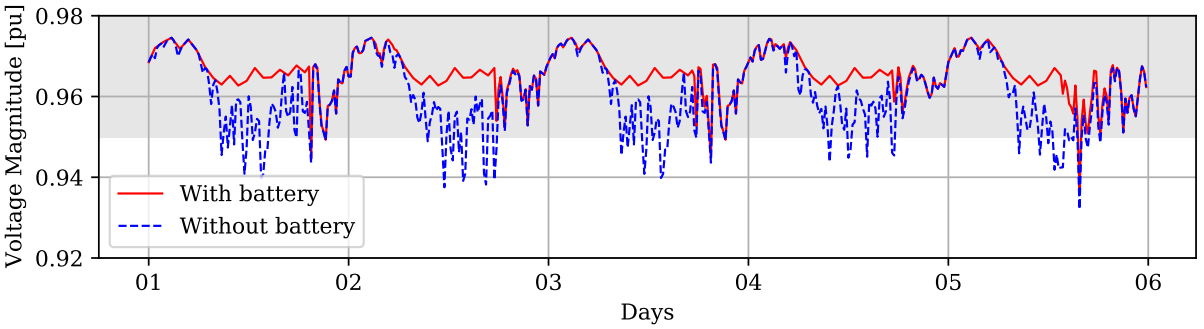

Figure 5.14: The voltage with and without battery with **rule-based control**. The minimum voltage is 0.936, which is an increase compared to the base case.

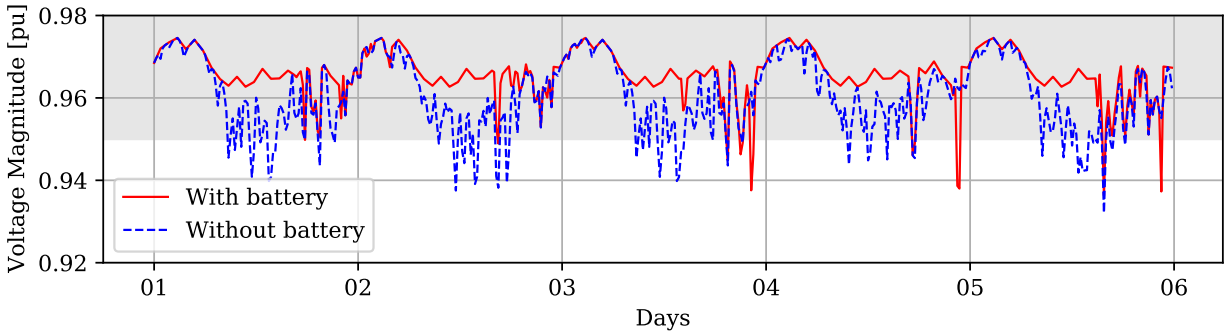

Figure 5.15: The voltage with and without battery with **optimization based control**. The minimum voltage is 0.936, which is an increase compared to the base case.

As seen from Table 5.5, the cost is lower with an optimization-based approach, which align with expectations. On days 3 and 4, the optimization-based control charges the battery with grid power right before midnight, causing significant voltage drops. With the given control of the battery, there is still a need for reactive power even when the production is the highest throughout the year.

Table 5.5: Voltage and cost results for the two control strategies with battery in the high production case.

High production case	**No battery**	**Rule-based**	**Optimization based**
Within voltage limits	98.3 %	99.0 %	97.5 %
Average deviation	$4.3 \cdot 10^{-3}$ pu	$5.1 \cdot 10^{-3}$ pu	$6.3 \cdot 10^{-3}$ pu
Minimum voltage	0.936 pu	0.936 pu	0.936 pu
Cost	4 230 NOK	2 821 NOK	2 741 NOK

5.3.2 Voltage Control with Reactive Power

The voltage results after the reactive power support is presented in Figure 5.16 and Figure 5.17. There are no significant voltage violations when the reactive power is used to compensate.

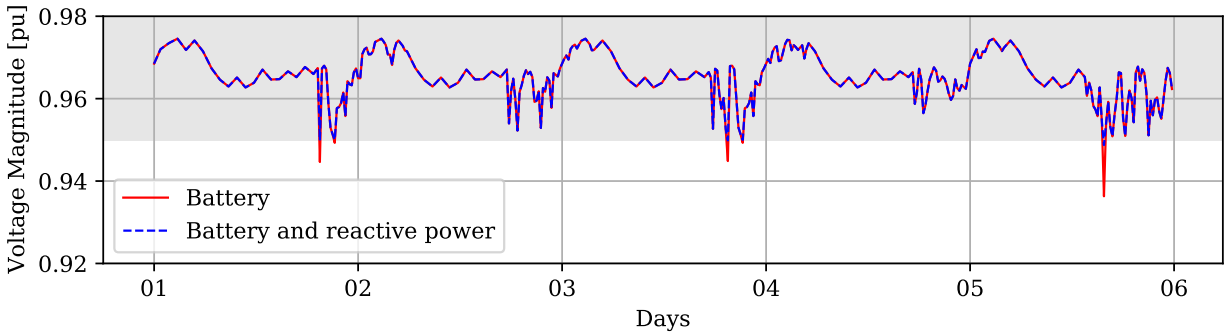

Figure 5.16: The voltage with and without reactive power support with the rule-based battery control. The minimum voltage is increased from 0.936 pu with battery to 0.949 pu with additional reactive power support.

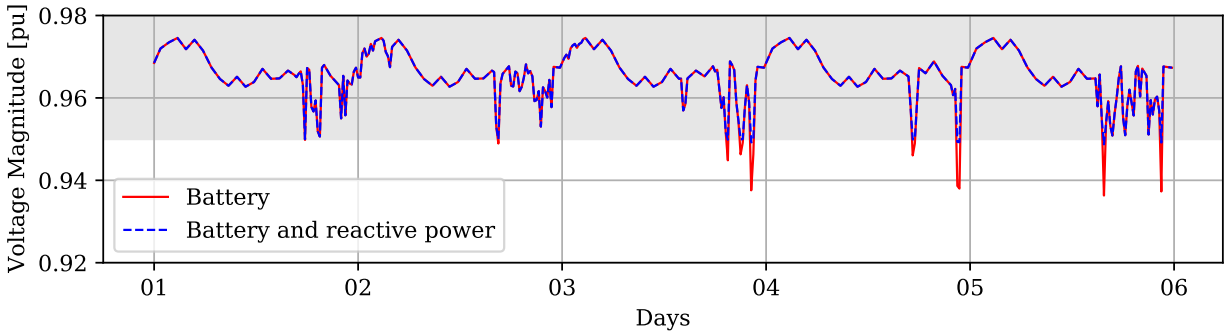

Figure 5.17: The voltage with and without reactive power support with the optimization based battery control. The minimum voltage is increased from 0.936 pu with battery to 0.949 pu with additional reactive power support.

The voltage, reactive power and energy cost results are presented in Table 5.6. The results verify that the system can sustain an acceptable voltage profile during a good production period. When the production is is high, the battery and PV have more impact on the voltage compared to the impact of reactive power, even though the battery operation does not consider the grid.

Table 5.6: Voltage and cost results for the two control strategies, where reactive power is used to compensate for voltage drops.

High production case	**No battery**	**Rule-based**	**Optimization based**
Within voltage limits	98.3 %	99.8 %	99.0 %
Average deviation	$0.22 \cdot 10^{-3}$ pu	$0.31 \cdot 10^{-3}$ pu	$0.36 \cdot 10^{-3}$ pu
Minimum voltage	0.949 pu	0.949 pu	0.949 pu
Reactive energy injected	1.04 MVArh	0.78 MVArh	2.52 MVArh
Cost	4 230 NOK	2 821 NOK	2 741 NOK

The rule-based control performs slightly better than the other cases when it comes to voltage, having the lowest deviation from the limit. However, on a cost basis, the optimization-based approach can reduce the energy costs by 35.2%, compared to not having a battery.

5.3.3 With Prediction Errors

Similar to the previous case, this section is meant to demonstrate the simple MPC-inspired battery control, taking into account the stochasticity of the load and production. Figure 4.4 and Figure 4.5 are the input for load and PV production in the algorithm, respectively. The summer profiles in Figure 4.5 are used in the high production scenario. Especially on days 3-5, there is a significant deviation between predicted and measured production. To deal with the deviations, the balancing algorithm in section 4 is implemented, and the results for the SOC are presented in Figure 5.18.

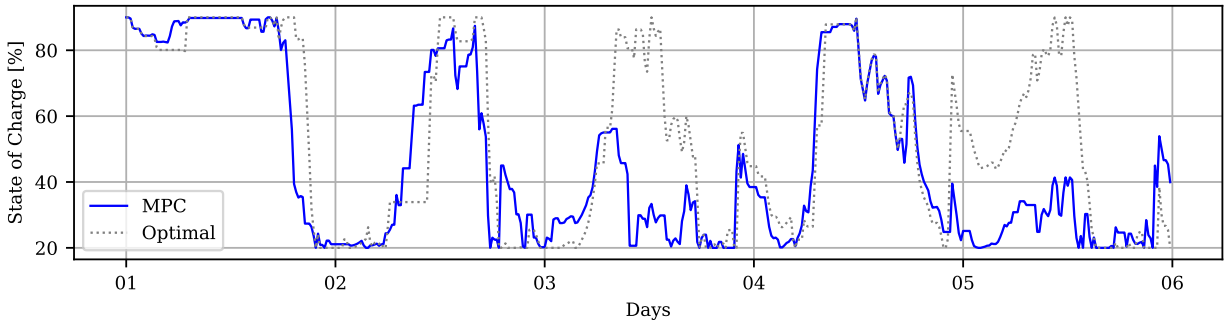

Figure 5.18: SOC of the battery during the summer when there is high production. The optimization happens with a shifting 24-hour horizon.

Table 5.7 presents the voltage- and cost results for the MPC-based control, for high production, with and without reactive power support. There is a significant improvement when it comes to both average deviation and minimum voltage when reactive power is used as additional support.

Table 5.7: Voltage and cost results for the system for the two control strategies.

MPC based	**Without reactive power**	**With reactive power**
Within voltage limits	97.5 %	99.2 %
Average deviation	$7.9 \cdot 10^{-3}$ pu	$0.45 \cdot 10^{-3}$ pu
Minimum voltage	0.936 pu	0.949 pu
Reactive energy injected	0 MVArh	2.92 MVArh
Cost	3 181 NOK	3 181 NOK

5.4 Sensitivity Analysis

A sensitivity analysis is conducted to see how changes in inputs impact the performance of the control strategies. This is done for the voltage limit, charging power limit, grid power limit, battery size, and load size. The intention is to analyze if any of the limitations and assumptions made in the modeling phase have a big impact on the results.

Impact of Upper Voltage Limit

In the simulated distribution grid, none of the buses inject active power to the grid. This means that no factors are causing the voltage to rise, other than reactive power injection at bus 10. However, in other systems, over-voltage might be an issue. To address this, the base case simulation was made, but with an upper bound on the voltage magnitude at 0.97 pu at bus 11, in addition to the existing lower bound of 0.95 pu. The results are presented in Figure 5.19. It can be seen from the figure that the control system can keep the voltage within the upper limit as well.

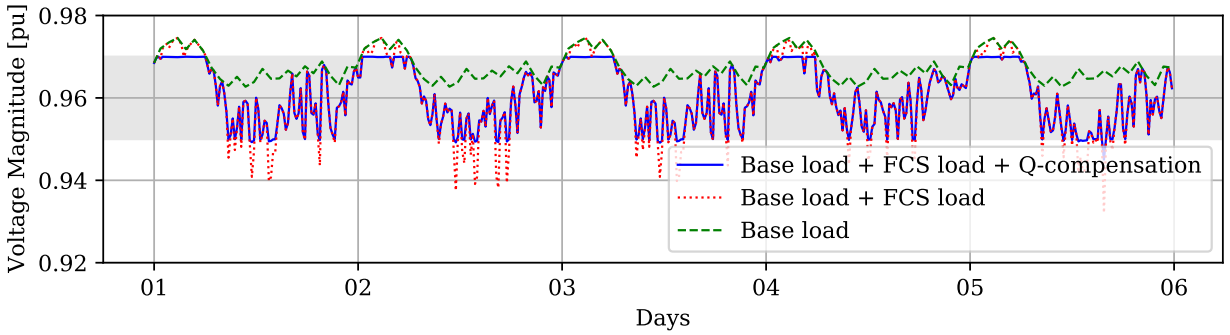

Figure 5.19: Reactive power control of the base case, with an additional upper limit on the voltage. The reactive power control is able to keep the voltage within the acceptable bound, which is the shaded area.

Impact of Charging Power Limit

The battery is programmed to optimize energy costs, and while this is beneficial for the charging station operator, the recharging of the battery during off-peak hours leads to significant voltage drops. To address this, the maximum power that the battery can charge is adjusted, to see if this has a positive impact on the grid. Also, it is interesting to see to which degree this constraint has an impact on the energy costs. The charging limit is set to be half the original charging power, giving a limit of 0.5 MW. The results are presented in Table 5.8. The results are from after the reactive power is provided, and it is for the low production scenario. Δ is related to the same simulation with a 1 MW charging power limit.

Table 5.8: Results from reducing the charging power limit from 1 MW to 0.5 MW. The results are from after the reactive power is provided, and it is for the low production scenario. Δ is related to the same simulation with 1 MW charging limit.

Charging Power Limit	**Rule-based**	Δ	**Optimization based**	Δ
Within voltage limits [%]	98.5 %	+0.0%	96.5 %	+2.7%
Average deviation [pu]	$0.24 \cdot 10^{-3}$	+0.0%	$0.70 \cdot 10^{-3}$	−57%
Minimum voltage [pu]	0.945	+0.0%	0.933	+0.1%
Injected RE [MVArh]	8.72	+0.1%	14.0	−27%
Cost [NOK]	18035 NOK	+0.0%	17659 NOK	+0.1%

It is clear from these results that the average deviation and reactive energy injected are reduced significantly when an optimization-based approach is used. The cost increase is quite low, respectively 0.1% and 0.0%. The rule-based control is not affected by the limit, because it is mostly empty, as seen from Figure 5.5. The minimal voltage is also increased, even though the change is not as significant as for the average deviation.

Impact of Grid Power Limit

Because a significant part of the electricity bill for the FCS operator is the capacity charge, which is decided by the peak power, it is relevant to use the battery for peak load reduction. So far, only the energy component has been considered in the cost optimization, however, it has been seen from the results that the charging of the battery causes significant peaks and associated voltage drops. It is therefore relevant to see the voltage

impact of putting a maximum power limit for grid imported power. The limit is set to 1.5 MW, which is the rating of the FCS. The results are presented in Table 5.9.

Table 5.9: Results from reducing the grid power limit to 1.5 MW. The results are from after the reactive power is provided, and it is for the low production scenario. Δ is related to the same simulation with no limit on the grid power.

Grid Power Limit	**Rule-based**	Δ	**Optimization based**	Δ
Within voltage limits [%]	87.3 %	−11.4%	86.9 %	−7.5%
Average deviation [pu]	$0.25 \cdot 10^{-3}$	+0.0%	$1.01 \cdot 10^{-3}$	−38%
Minimum voltage [pu]	0.945	+0.0%	0.945	+1.5%
Injected RE [MVArh]	8.72	+0.0%	20.5	+6.8%
Cost [NOK]	18 035 NOK	+0.0%	17 650 NOK	+0.0%

It can be seen from the table that putting an upper limit on the imported grid power, reduces the average deviation from the limit, without impacting the costs. Similar to when the charging power was reduced, the rule-based control is not affected by the limit. This, therefore, seems like an attractive choice for both the FCS operator and the DSO. When the peak loads are reduced, the available reactive power can compensate to a much larger degree.

Impact of Battery Size

Because there is no optimization involved in the choosing of battery size in this thesis, it is interesting to see to which extent the battery size impacts the performance. This sensitivity analysis is conducted for two different battery sizes, ±50% of the original battery size of 1 MWh. All the other inputs are kept constant, including the maximum charging power. Table 5.10 and Table 5.11 presents the main results from this analysis. The simulation is run for each of the battery sizes, and the time horizon is five days.

Table 5.10: Results from reducing the battery size to 0.5 MWh. The results are from after the reactive power is provided, and it is for the low production scenario. Δ is related to the same simulation with 1 MWh battery.

Reduced battery size	**Rule-based**	Δ	**Optimization based**	Δ
Within voltage limits [%]	98.5 %	+0.0%	95.4 %	+1.6%
Average deviation [pu]	$0.24 \cdot 10^{-3}$	−0.9%	$1.8 \cdot 10^{-3}$	+11%
Minimum voltage [pu]	0.945	+0.0%	0.931	+0.0%
Injected RE [MVArh]	8.86	+1.6%	16.2	−15%
Cost [NOK]	18 205 NOK	+0.9%	18 008 NOK	+2.0%

Table 5.11: Results from increasing the battery size to 1.5 MWh. The results are from after the reactive power is provided, and it is for the low production scenario. Δ is related to the same simulation with 1 MWh battery.

Increased battery size	**Rule-based**	Δ	**Optimization based**	Δ
Within voltage limits [%]	87.5 %	−11.2%	86.9 %	−7.5%
Average deviation [pu]	$0.25 \cdot 10^{-3}$	+1.4%	$1.8 \cdot 10^{-3}$	+12%
Minimum voltage [pu]	0.945	+0.0%	0.931	−0.1%
Injected RE [MVArh]	8.63	−0.1%	18.8	−2.2%
Cost [NOK]	17 864 NOK	−0.9%	17 307 NOK	−2.0%

In contrast to the previous sensitivity analyses, the rule-based results are affected by the battery size. The influence on voltage results is more significant for the optimization-based control. Here, the average deviation from the voltage limit is increased, both with reduced and increased battery size. The costs are reduced when increasing the battery size and opposite when decreasing the battery size, which also aligns with expectations.

Impact of Load Size

The system is tested with increased load size, to see if the system would withstand increased charging powers or EV share on the roads. The simulation was run with a load profile with a 45% increase from the original scenario, amounting to 50.1 MWh. The results from this simulation are presented in table Table 5.12.

Table 5.12: Results from increasing the load by 45%, from 34.5 MWh to 50.1 MWh. The results are from after the reactive power is provided, and it is for the low production scenario. Δ is related to the same simulation with 34.5 MWh load.

Increased battery size	**Rule-based**	Δ	**Optimization based**	Δ
Within voltage limits [%]	92.5 %	-6.1%	89.6 %	-4.7%
Average deviation [pu]	$1.1 \cdot 10^{-3}$	$+362\%$	$3.7 \cdot 10^{-3}$	$+268\%$
Minimum voltage [pu]	0.934	-1.2%	0.910	-3.7%
Injected RE [MVArh]	24.0	$+175\%$	29.8	$+56\%$
Cost [NOK]	26 472 NOK	$+47\%$	26 072 NOK	$+48\%$

The control strategies are quite sensitive to an increase in load, especially when it comes to average deviation and injected reactive energy. It can be seen that the amount of reactive power is increasing significantly in all the simulations and that the voltage and reactive power for the rule-based control is the most sensitive to the increased load, compared to the other control strategies. The impact on costs is quite similar for the two control strategies.

Chapter 6

Discussion

The following chapter discusses the findings from the results section, focusing on the modeling and operational results. The chapter has a similar structure as the results section. First, each of the operational scenarios from the previous chapter is discussed, where the focus is the ability to reduce costs and keep the voltage within acceptable limits. The operational aspect is followed by a discussion of the sensitivity results, focusing on the learning outcome from the analysis. Further, the modeling approach is discussed, highlighting both weaknesses and strengths in the chosen control strategies, as well as assumptions and limitations. The chapter is concluded with a recommendation for further work, based on the gained insight of the discussion.

6.1 Operation

In this section, each of the operational scenarios is discussed, where the focus is on the system's ability to reduce costs and keep the voltage within acceptable limits. The discussion will mirror the results. For the base case, the results will be discussed on a voltage- and cost basis. For the low- and high production scenarios, the discussion will provide insights on the battery operation and voltage support, comparing the control strategies on a voltage and cost basis.

6.1.1 Base Case

The base case aims to highlight how the system would behave if a control strategy was used for providing reactive power support with FCS alone. Results from the base case, as presented in Figure 5.2, show that the voltage is closer to the limit of 0.95 by introducing reactive power support from the FCS, however, there are still some violations, especially in the middle of the day. There are different ways to analyze the results from this case. First, the focus can be on the average deviation from the voltage limit of 0.95 pu. Even though the voltage is within the limits for the same amount of time with and without reactive power, the average deviation from the limit is reduced from 0.0047 to 0.00066 pu. This is a substantial decrease that shows the benefit of reactive power injection. The reactive power is supplied from the FCS converter, as designed. It is demonstrated that having additional support from the PV inverter is important for the highest peak loads. This augments the advantage of having a system that includes local production, as the inverter can be utilized even where there is no production. However, there are critical time steps during which reactive power injection is not able to correct the voltage deviations as illustrated in Figure 5.2. This occurs due to the limited rating of the converter. The load at this timestep is high, which takes up most of the capacity of the FCS converter, leaving little capacity for reactive power injection. As seen from Figure 5.3, the reactive power from the PV inverter has a peak at this timestep. However, this amount of reactive power is not sufficient to correct the voltage. During the timesteps where the voltage is corrected, the voltage is not precisely corrected to 0.95 pu. This is most likely due to the linearization in the power flow, around the operating point, which could lead to deviations especially when the voltage drop is high.

Another way to analyze these results is on a cost basis. As seen from Table 5.1, the cost is equal both with and without reactive power as reactive power does not have a direct market effect. Nevertheless, it is important to separate day-to-day operation and long-term planning when it comes to costs. Aspects such as lifetime reduction of the power electronics could also be a disadvantage to using reactive power. A life-cycle analysis of the components are not within the scope of this thesis, however, an overall cost-benefit analysis including this would be essential, especially as a decision basis for investing in the relevant control systems.

6.1.2 Low Production Case

The low production case is meant to highlight how the system behaves when there is close to zero production, but still high load. The following paragraphs will discuss the results for the battery operation and voltage control, and compare the control strategies on a voltage and cost basis.

The operation of the battery is shown to be very dependent on the control strategy, as it can be observed from Figure 5.5. The rule-based control strategy is not able to utilize the battery potential, and the impact of the

battery is almost negligible. On the other hand, the optimization-based control can charge the battery from the grid, and the battery is therefore utilized to a larger extent. The battery is operated to minimize energy costs, and there is no upper limit on the grid power. Therefore, the battery charging causes significant voltage drops. It can therefore be argued that this is against the purpose of the battery. However, from the FCS operator's perspective, who is not directly interested in the grid condition, an optimization-based control seems like the more attractive option. As seen from Table 5.2, the energy costs are lowest when using the optimal controller, which aligns with expectations.

On the other hand, the DSO is not contented with these control strategies alone, as this leads to higher voltage drops and peak loads. That leads to the use of reactive power control. It can be seen from from Figures 5.8 and 5.9 that the voltage is at the given limit of 0.95 pu to a larger extent. The reactive power can correct the voltage drops caused by the stationary battery. However, similar to the base case, there are some instances, where the reactive power is not sufficient to correct the voltage to 0.95 pu. The critical times where this happens are when the battery is charging from the grid at maximum power, and the FCS load is high. Even though some voltage drops are not corrected, the average deviation from the voltage limit is lower than for the base case for all the control strategies. The rule-based control even has a lower voltage limit deviation than the base case with reactive power compensation.

When comparing the two control strategies, it is clear that with the given system, the optimal battery control is the most appealing for the FCS operator, as it reduces energy costs. The rule-based control is found to be the most efficient for the voltage situation, however, the system would be performing almost the same way without the battery. The battery is not able to recharge once it is empty, which is to be expected during the winter when there are many consecutive days of low production. With that said, the battery would be almost empty for a significant portion of the year, which is not favorable when an investment is made. On the other hand, other cost aspects must be considered that are not included in the optimization. This is for example capacity charge, which could increase the cost of the optimization-based controller with the given objective and constraints. Another cost aspect that can be discussed, is the required reactive power. It should also be considered that the amount of reactive energy injected is more than double when using the optimal control, compared to using the rule-based control or not having a battery at all. This could in turn lead to higher strain on the converter, and indirect costs due to lifetime reduction or maintenance. This aspect should be considered in a life-cycle analysis.

When prediction errors are introduced, it is expected that the system has a sub-optimal performance. Figure 5.11 show that the MPC-based controller can follow the optimal trajectory to a certain extent. Similar to the optimal battery control, the battery operations lead to high voltage drops and resulting in an average deviation from the limit of 0.0078 pu. When introducing reactive power support, the average deviation reduces to 0.00074 pu, which is significant. This implies that even if there were deviations between predictions and measured powers the system is still able to sustain a good voltage profile when reactive power is used. It, therefore, leads to more freedom when it comes to objective functions for the battery and less precise and computationally expensive predictive algorithms. However, to maximize the benefit of the FCS operator, the predictions should be as good as possible to have optimal performance. Moreover, it is good to know that reactive power control can be a security if the predictions are not precise.

6.1.3 High Production Case

The high production case is meant to highlight how the system behaves when production is very high during the summer. Results show that during a good production period, the system can sustain a good voltage profile. The following paragraphs will discuss battery operation and voltage control, and compare the control strategies on a voltage and cost basis.

As expected, the system is performing much better when there are many consecutive days of high production. When it comes to battery operation, the voltage is less influenced by the battery charging than the low production scenario. This is expected, as the PV power can contribute to charging the battery. It is also observed that the battery operation across the strategies is more alike, especially in terms of SOC. This is due to the PV power, which is also used to charge the battery. The main difference in the SOC of the control strategies is that the optimization-based control charges the battery with power from the grid before midnight when the prices are low, causing significant voltage drops at these hours. However, overall, the voltage profile is above limit to a larger extent, as seen from Figures 5.14 and 5.15. The main aspect of this operational situation is the cost reduction because the voltage profile is satisfactory with all the strategies. And on a cost basis, the optimization-based control is the strategy that performs best, reducing the energy costs by 35.2% compared to not having a battery. On the other hand, this controls strategy demands a lot more reactive power from both the PV and FCS, which is an additional strain on the components and can cause increased losses.

When comparing the two control strategies, the optimization-based control performs better than the rule-based in terms of cost and keeps the voltage within limits to a larger extent. The battery and PV production is the main contributor to keeping the voltage within limits, however, reactive power is also necessary to meet the voltage requirements. All in all, the system can deliver the desired value to both the FCS operator and the DSO, with both control strategies. This is expected as this is not a critical operational situation, such as the previous case.

It is quite evident from Figure 5.18 that the measured production is lower than predicted, and the battery is therefore discharged to compensate for the lack of production. Similar to the low production case, it is demonstrated that even with sub-optimal performance, the voltage can stay within limits to a much higher degree. Thus, the requirement for the DSO is met, and for the FCS operator to be content, the predictions must have the highest possible precision.

6.2 Sensitivity to Inputs

As demonstrated in the results, the system is affected by a change in inputs. One of the main findings from the sensitivity analysis was that limiting either the maximum charging power or imported grid power could lead to increased benefits for both the DSO and the charging station operator. For the DSO, the main benefit is the improved voltage profile due to lower peak loads. The charging station operator could benefit in multiple ways, the first is reduced capacity charge due to reduced peak load, second is less strain on the components, which could reduce battery deterioration, and thereby reducing the increased losses and lifetime reduction of utilizing reactive power from the FCS converter or PV inverter.

When it comes to the battery size, there are some expected results and some that are more interesting. It is expected that the cost are quite ”linear” in terms of increase/decrease in battery size. An interesting result is that both increasing and decreasing the battery size by 50% leads to an increase in deviation from the voltage limit. This implies that the chosen battery size is well fit for the system when it comes to size. In addition, from an FCS operator perspective, an increased battery size leads to reduced energy costs, but it could be discussed if this would justify the increased investment cost.

The load size impact can also be discussed. An increase in load size has a significant impact. Due to the increase in EV share that is expected in the close future, this is a relevant issue that should be considered when planning an FCS. One interesting observation is that even with this 45% increased load, the average voltage deviation from the limit was smaller than for the base case in all control systems. This emphasizes that the combination of local production, battery, and reactive power control creates the potential for the FCS to increase the number of charging outlets or the charging power. However, the minimum voltage is quite low for the optimization-based control, and it is close to the limit of the regulation. If this was the load situation, grid power or charging power limit could be introduced. This has been demonstrated to have a positive influence on the voltage without influencing the costs too much. On a general note, even though the rule-based approach shows better results in terms of voltage, the flexibility of the optimization-based approach is important to address. The constraints can easily be altered to fit the needs of the system, which is emphasized in this sensitivity analysis.

6.3 Shortcomings and Strengths

This subsection provides a critical perspective on the modeling in this thesis and highlighting its strengths. The discussed modeling aspects are inputs, grid model, rule-based model, optimization model, and MPC model.

Inputs

When analyzing the controllers, it is important to keep in mind the type of load which is analyzed. FCS load is intermittent and with high peaks, on top of the fact that the charging power on the market is increasing. It is a known fact that the FCS load is not easily predictable, and it could be difficult to foresee the demand for reactive support for future time steps. In this thesis, the load, production, and spot prices are assumed to be completely deterministic for the rule- and optimization-based controllers. In reality, this is not the case, but intelligent prediction models could help to achieve more optimal control. When it comes to the MPC model inputs, the load and production are non-deterministic, in the sense that the controller is adjusting the control actions according to prediction errors. However, these predictions are not updated for each timestep, which is what would happen if a prediction algorithm was in place. The method is therefore successfully demonstrating how the balancing works, and it could be combined with a prediction algorithm to improve the results. In addition, the load used in this thesis is not measured data, the load data used is just used to get a realistic load profile, based on factors such as traffic flow, charging time, and so on. However, the load profiles used can illustrate a realistic load situation in the distribution grid, which is essential to validate the proposed control strategies.

Another aspect of the modeling inputs is the length of the time steps. The output data from the stochastic load modeling was given in minutes. However, using minute resolution would make the simulations 15 times more computationally expensive. To put it in perspective, simulating a day with minute resolution gives 1440 time steps, meaning 1440 individual operations of the controllers. Using a 15 minute time step for five days gives 480 timesteps. Because it was considered more valuable for the analysis to have a longer horizon, the sacrifice of the high data granularity was made. A possible drawback of this is that the 15-minute data does not capture if there are higher peaks on a minute level. This means that there could be even higher peaks and associated voltage drops than what is observed in the simulation. On the other hand, if the control was applied in real-time, the algorithm is fast enough to be executed within a minute. Nevertheless, for this thesis, a faster run time was prioritized.

Grid model

As mentioned in section 3, the distribution transformer was omitted in the model. In addition, other assumptions were made, such as the size of the grid components and the daily base load. It is important to emphasize that the grid model is not based on actual customer data. The system with the given simplifications would deviate from the physical system if there was a similar system in real life. However, the aim of this work is mainly to develop a methodology, which could be applied to other systems and grid models as well. Therefore, the simplifications have not in any way limited the purpose of this work.

Rule-Based Controller

The rule-based battery control was shown to have many weaknesses in the simulations. First of all, it is not able to operate in a way that accounts for the future timesteps, due to the rule-based nature of the controller. As mentioned in the controller description, this controller was not able to charge from the grid, as an attempt to minimize the grid imported power. And to a certain extent, it can be said that this was achieved, however, from an FCS operator's perspective, the motivation for minimizing the grid imported power is to minimize cost. Due to the daily variations in spot prices, minimizing grid power does not necessarily mean lower costs, as it depends on the timing as well. In addition, by not allowing the battery to charge from the grid, the battery is not able to recharge, which is not beneficial for the investor. This is probably the biggest drawback of the rule-based controller. A possible solution is to expand the control algorithm to charge the battery when the price is below a certain threshold. In this way, the operation might be closer to the optimal control. However, this control strategy does not account for future timesteps, so it will not achieve optimality.

Optimization Model

The optimization model was able to minimize costs. The strength of the proposed optimization model is that the objective function easily could be changed to fit the aim of the FCS. This could for example be to limit the overall power imported from the grid. The flexibility of this optimization model has been illustrated in the sensitivity analysis, and the constraints and objectives could easily be altered. The main shortcoming of the optimization model is that it does not consider the grid in any way. This leads to high peaks in the middle of the day, when the prices have a slight drop, which has a serious voltage impact. A way to address

this is by introducing a constraint with an upper limit on the grid power, where the limit is decreased under constrained conditions. This would encourage the battery to spread the charging of the battery throughout the day, and not have the high peaks in the middle of the day. The system could also benefit from include other cost elements in the objective function, such as grid tariffs, degradation costs, and investment costs. In this way, the battery could be operated more optimally, as more information is included. Another way to address that the battery control does not consider the grid is by implementing a joint controller for reactive power and battery. In this way, the battery could minimize costs, while being constrained by grid constraints.

MPC Model

The MPC model includes a sub-controller that balances the powers if the measurements deviate from the predictions. This is done in a rule-based manner where the battery is the main source of balancing. However, the balancing algorithm could be improved both when it comes to cost and voltage operation. This is because the straightforward balancing of the errors leads to sub-optimal performance, as it does not consider costs. This would have an increasing impact with higher deviations. As mentioned, the nature of the FCS load makes it hard to predict. However, using machine learning or other predictive tools, the predictions could be potentially improved and the power balancing might not have such an impact on the results. In other words, the key for this algorithm to work optimally is to have high precision forecasts for the FCS load and production. It is important to address the relevance of this controller. As the inputs are not deterministic, the control system must have a strategy for dealing with deviations. If there is not, and the powers are dispatch without adjustments to real-time powers, it could lead to frequency issues in the grid. A good strategy for balancing these deviations is vital, especially when the forecasts available are precise.

Another shortcoming of the MPC model is that the predictions are fixed, and the same predictions are used throughout the optimization horizon. Ideally, the predictions should be dynamic, because the deviation that happened in time step t might affect what happens in the next timesteps. This is especially relevant for fast charging, because the EV is most likely charging for longer than 15 minutes, and it would therefore affect more than one timestep. With that said, this requires advanced prediction algorithms which are out of scope for this thesis. However, it could be expected that with a full-fledged MPC control, the deviations would not be as large as they are in this thesis, and the performance would be better and more close to optimality.

This MPC model was not directly compared to the two other battery controllers as they were tested with different inputs, and it would be an unfair comparison, especially when it comes to costs. If the rule- and optimization-based controllers had the same non-deterministic inputs and subsequent balancing algorithms, it would have been possible to compare the strategies directly. However, that was not within the scope of this thesis.

Reactive Power Control

The two-step approach to the control of battery and reactive power is fitting for a system where the forecast precision is low. This is because the introduction of a joint optimization function for the battery and reactive power would increase the computational expense substantially. For a system with low precision, a joint optimization function would be redundant, in the sense that the system would still deviate from predictions. Therefore, it could be reasoned that it is sufficient to have a two-step control approach. However, the reactive

power controller could be improved by controlling the reactive power with an MPC, such as in [10].

A shortcoming of the reactive power controller is that there is no secondary voltage control is the reactive power capacity is not sufficient. Even though the PV inverter leads to a sufficient increase in capacity, there is still a limitation in the PV inverter and FCS converter ratings. Therefore, as it has been seen from the results, some of the highest peaks will not have enough capacity to reach the voltage limit. A possible solution to this would be to have additional reactive power from the battery converter, or injecting active power from the PV or battery, or by limiting the charging power during critical hours.

6.4 Further Work

The designed methodology has room for multiple improvements which could be explored in future research. For example, when it comes to modeling, the battery controllers have a lot of potential for development. An example is expanding the objective function in the optimization-based controller to include other cost elements, such as grid tariffs and degradation costs. If an investment cost were included as well, an optimal battery size could be found. A longer horizon could also be implemented. Having a horizon of e.g. a year, the results would give a more comprehensive insight into the system behavior over time. The control strategy in this thesis could also be combined with the approach in [10], where the proposed MPC controller could be used to schedule the battery and the MPC in [10] could be used to control the reactive power.

When it comes to grid modeling, the model could be improved by including reactive power of the base load, and it would be valuable to see the impact PV- or battery power injection would have on the voltage. Especially because the simulated distribution grid in this thesis only included load buses. This could for example be done by modeling another grid with other characteristics. It could also be interesting to explore other ways that this type of system could provide services to the grid. For example by increasing the reactive power capacity by providing reactive power from the battery converter, active power support by curtailing the FCS load, or injecting power from the battery or PV.

Another recommendation would be to expand the economic analysis done in this report, by including investment costs of components and control systems. It would also provide great insight if the aspect of reactive power costs were included, as this could have an impact on the results. Including revenues from injecting power produced by the PV would also be interesting to include. To increase the benefit further, the potential for the battery to provide multiple services could be investigated, such as frequency containment, or participation in local flexibility markets. From an FCS operator's point of view, this additional revenue could act as an incentive for investing in flexible resources.

Chapter 7

Conclusion

In this master's thesis, a methodology for voltage support from a fast charging station has been developed. This includes three control strategies namely, a rule-based, optimization-based, and an MPC-based battery control, together with a reactive power control based on voltage sensitivity calculations. To verify the control strategies, simulations were carried out on a system consisting of a fast charging station equipped with 10 charging outlets of 150 kW rating each, a 1 MWh stationary battery, and a 1.38 MWp PV system. The control strategies were simulated for a base case, low production scenario, and high production scenario.

In a low production scenario, the rule-based control strategy does not utilize the potential of the battery. With an optimization or MPC-based control, the battery recharges when the prices are low, which leads to peak loads and associated voltage drops. However, combined with reactive power, the voltage drop is mitigated. The reactive power is therefore the main contributor to the improved voltage profile. In a high production scenario, the results verify that the system can sustain an acceptable voltage profile. The battery and PV production are the main contributors to keeping the voltage close to the limit, and the main difference between the rule- and optimization-based controllers is the cost reduction of the optimal control.

In addition to the operational results, the versatility of the model has been demonstrated through a sensitivity analysis. It is found that the proposed control system gives better voltage results with a 45% higher load, compared to the voltage if there was original load and no battery or PV. By reducing the charging power limit from 1 MW to 0.5 MW, the average voltage deviation from the limit was reduced by 57%, for a 0.1% increase in costs. Limiting the grid power to 1.5 MW resulted in a 38% reduction in voltage deviation, without any noticeable increase in cost. The developed control strategy, therefore, allows higher charging powers for the charging station operators, and limited grid impact for the grid operators. The results also illustrate that the utilization of reactive power can provide voltage support when the battery has a sub-optimal performance due to prediction errors, and could therefore allow less computationally expensive prediction algorithms.

To address the research questions stated in the introduction, the optimal battery control strategy for the FCS operator is an optimization-based control. However, if the proposed battery controllers were to be implemented in practice, they should either account for grid tariffs or have an upper limit on charging power or grid imported power. A good strategy for voltage support with reactive power is by utilizing both the FCS converter and PV inverter, but there is a need for some secondary voltage support when the reactive power capacity is not sufficient. It is concluded that the voltage at the critical bus can be improved considerably by using reactive power. By combining this with a stationary battery and local production, it can also increase benefit for the charging operator.

References

[1] DNV GL. “Energy Transition Outlook - Power Supply & Use 2020”. In: (2020), p. 84.

[2] IEA. *Global EV Outlook 2020 – Analysis*. IEA. URL: https://www.iea.org/reports/global-ev-outlook-2020.

[3] Samferdselsdepartementet. *Nasjonal transportplan 2022-2033*. Regjeringen.no. Publisher: regjeringen.no. Mar. 19, 2021. URL: https://www.regjeringen.no/no/dokumenter/meld.-st.-20-20202021/id2839503/.

[4] *Ladestasjoner*. URL: https://elbil.no/elbilstatistikk/ladestasjoner/.

[5] *Nasjonal transportplan: - Mangler plan for lading*. URL: https://elbil.no/nasjonal-transportplan-mangler-plan-for-lading/.

[6] Martin Lillebo et al. “Impact of large-scale EV integration and fast chargers in a Norwegian LV grid”. In: *The Journal of Engineering* 2019.18 (July 1, 2019), pp. 5104–5108. ISSN: 2051-3305. DOI: 10.1049/joe.2018.9318.

[7] Sven Kalker et al. “Fast-Charging Technologies, Topologies and Standards”. In: vol. 10. E.ON Energy Research Center Series, 2018.

[8] Simon Funke et al. “Fast charging stations with stationary batteries: A techno-economic comparison of fast charging along highways and in cities”. In: *Transportation Research Procedia*. Recent Advances and Emerging Issues in Transport Research – An Editorial Note for the Selected Proceedings of WCTR 2019 Mumbai 48 (Jan. 1, 2020), pp. 3832–3849. ISSN: 2352-1465. DOI: 10.1016/j.trpro.2020.08.036.

[9] *How battery storage can help charge the electric-vehicle market*. McKinsey. URL: https://www.mckinsey.com/business-functions/sustainability/our-insights/how-battery-storage-can-help-charge-the-electric-vehicle-market.

[10] J. R. A. Klemets and B. N. Torsæter. “MPC-based Voltage Control with Reactive Power from High-Power Charging Stations for EVs”. In: *2021 IEEE Madrid PowerTech, [To be published]*.

[11] Ivan Pavić, Tomislav Capuder, and Igor Kuzle. “Fast charging stations — Power and ancillary services provision”. In: *2017 IEEE Manchester PowerTech*. 2017 IEEE Manchester PowerTech. June 2017, pp. 1–6. DOI: 10.1109/PTC.2017.7981190.

[12] V. Monteiro et al. “Assessment of a battery charger for Electric Vehicles with reactive power control”. In: *IECON 2012 - 38th Annual Conference on IEEE Industrial Electronics Society*. IECON 2012 - 38th Annual Conference on IEEE Industrial Electronics Society. ISSN: 1553-572X. Oct. 2012, pp. 5142–5147. DOI: 10.1109/IECON.2012.6389554.

[13] Sumit Paudyal et al. “Optimal coordinated EV charging with reactive power support in constrained distribution grids”. In: *2017 IEEE Power & Energy Society General Meeting*. 2017 IEEE Power & Energy Society General Meeting (PESGM). Chicago, IL: IEEE, July 2017, pp. 1–5. ISBN: 978-1-5386-2212-4. DOI: 10.1109/PESGM.2017.8274266.

[14] Ioannis Lymperopoulos et al. “Ancillary Services Provision Utilizing a Network of Fast-Charging Stations for Electrical Buses”. In: *IEEE Transactions on Smart Grid* 11.1 (Jan. 2020). Conference Name: IEEE Transactions on Smart Grid, pp. 665–672. ISSN: 1949-3061. DOI: 10.1109/TSG.2019.2927701.

[15] DNV GL. “Batterier i distribusjonsnettet”. In: (Dec. 18, 2017).

[16] Hanne Sæle et al. *Fremtidens fleksible distribusjonsnett - Fleksibel nettdrift, forbrukerfleksibilitet, plusskunder og forretningsmodeller*. Accepted: 2016-08-24T12:13:07Z. SINTEF Energi AS, 2016. ISBN: 978-82-594-3648-1. URL: https://ntnuopen.ntnu.no/ntnu-xmlui/handle/11250/2402809.

[17] Naasir Ansar. *REACTIVE POWER SUPPLY FROM PV INVERTERS IN DISTRIBUTION NETWORKS*. Nov. 27, 2019.

[18] Ida Langseth. “Energy Management System for an Electric Vehicle Fast Charging Station”. In: (Dec. 2020), p. 65.

[19] *FuChar*. FuChar Project Website. URL: https://www.sintef.no/projectweb/fuchar/.

[20] *IONITY - TECHNOLOGY*. URL: https://ionity.eu/en/design-and-tech.html.

[21] Omer Turksoy, Unal Yilmaz, and Ahmet Teke. *Overview of battery charger topologies in plug-in electric and hybrid electric vehicles*. May 11, 2018.

[22] *150+ kW fast chargers*. Fastned. URL: https://support.fastned.nl/hc/en-gb/articles/115015420127-150-kW-fast-chargers.

[23] A. Zidan and H. A. Gabbar. “Chapter 8 - Design and control of V2G”. In: *Smart Energy Grid Engineering*. Ed. by Hossam A. Gabbar. Academic Press, Jan. 1, 2017, pp. 187–205. ISBN: 978-0-12-805343-0. DOI: 10.1016/B978-0-12-805343-0.00008-5.

[24] *Introducing V3 Supercharging*. Tesla. Mar. 6, 2019. URL: https://www.tesla.com/no_NO/blog/introducing-v3-supercharging.

[25] *CHAdeMO 3.0 released: the first publication of ChaoJi, the new plug harmonised with China’s GB/T*. Chademo Association. URL: https://www.chademo.com/chademo-3-0-released/.

[26] *Electric Vehicle Charging Overview*. Clean Vehicle Rebate Project. Nov. 29, 2018. URL: https://cleanvehiclerebate.org/eng/ev/technology/fueling/electric.

[27] *Nett - NVE*. URL: https://www.nve.no/energiforsyning/nett/?ref=mainmenu.

[28] *Regulation of grid operations*. Energifakta Norge. URL: https://energifaktanorge.no/en/regulation-of-the-energy-sector/regulering-av-nettvirksomhet/.

[29] Henning Taxt. *ELK-11 Cost-benefit analysis in distribution network planning*. PLANLEGGING AV DISTRIBUERT PRODUKSJON. Oct. 8, 2020.

[30] C.H. Dharmakeerthi, Mithulananthan Nadarajah, and Tapan Saha. *Overview of the impacts of plug-in electric vehicles on the power grid*. Journal Abbreviation: Innovative Smart Grid Technologies Asia (ISGT), 2011 IEEE PES Publication Title: Innovative Smart Grid Technologies Asia (ISGT), 2011 IEEE PES. Nov. 1, 2011. DOI: 10.1109/ISGT-Asia.2011.6167115.

[31] K. Clement-Nyns, E. Haesen, and J. Driesen. "The Impact of Charging Plug-In Hybrid Electric Vehicles on a Residential Distribution Grid". In: *IEEE Transactions on Power Systems* 25.1 (Feb. 2010). Conference Name: IEEE Transactions on Power Systems, pp. 371–380. ISSN: 1558-0679. DOI: 10.1109/TPWRS.2009.2036481.

[32] E. Sortomme et al. "Coordinated Charging of Plug-In Hybrid Electric Vehicles to Minimize Distribution System Losses". In: *IEEE Transactions on Smart Grid* 2.1 (Mar. 2011). Conference Name: IEEE Transactions on Smart Grid, pp. 198–205. ISSN: 1949-3061. DOI: 10.1109/TSG.2010.2090913.

[33] *Kraftmarkedet*. Energifakta Norge. URL: https://energifaktanorge.no/norsk-energiforsyning/kraftmarkedet/.

[34] *Endringer i nettleiestrukturen*. In collab. with Andreas Bjelland Eriksen et al. 2020. URL: http://publikasjoner.nve.no/rme_hoeringsdokument/2020/rme_hoeringsdokument2020_01.pdf.

[35] Joseph Stekli, Linqnan Bai, and Umit Cali. "Pricing for Reactive Power and Ancillary Services in Distribution Electricity Markets". In: *2021 IEEE Power Energy Society Innovative Smart Grid Technologies Conference (ISGT)*. 2021 IEEE Power Energy Society Innovative Smart Grid Technologies Conference (ISGT). ISSN: 2472-8152. Feb. 2021, pp. 1–5. DOI: 10.1109/ISGT49243.2021.9372202.

[36] A.A. El-Keib and X. Ma. "Calculating short-run marginal costs of active and reactive power production". In: *IEEE Transactions on Power Systems* 12.2 (May 1997). Conference Name: IEEE Transactions on Power Systems, pp. 559–565. ISSN: 1558-0679. DOI: 10.1109/59.589604.

[37] Masoud Aliakbar Golkar and Mahsa A. Golkar. *Reactive power pricing in deregulated electricity market*. Pages: 4. July 11, 2009. 1 p. DOI: 10.1049/cp.2009.0536.

[38] Pau Lloret et al. "Challenges in distribution grid with high penetration of renewables". In: (June 2017), p. 50.

[39] Mithat Can Kisacikoglu. "Vehicle-to-grid (V2G) Reactive Power Operation Analysis of the EV/PHEV Bidirectional Battery Charger". In: *Doctoral Dissertations* (May 1, 2013). URL: https://trace.tennessee.edu/utk_graddiss/1749.

[40] K. Wali, R. Koubaa, and L. Krichen. "Cost benefit smart charging schedule for V2G applications". In: *2019 16th International Multi-Conference on Systems, Signals Devices (SSD)*. 2019 16th International Multi-Conference on Systems, Signals Devices (SSD). ISSN: 2474-0446. Mar. 2019, pp. 34–39. DOI: 10.1109/SSD.2019.8893171.

[41] Xinzhou Li et al. "A cost-benefit analysis of V2G electric vehicles supporting peak shaving in Shanghai". In: *Electric Power Systems Research* 179 (Feb. 1, 2020), p. 106058. ISSN: 0378-7796. DOI: 10.1016/j.epsr.2019.106058.

[42] Wesley Cole and Allister Frazier. *Cost Projections for Utility-Scale Battery Storage: 2020 Update*. NREL/TP-6A20-75385, 1665769, MainId:6883. June 12, 2020, NREL/TP–6A20–75385, 1665769, MainId:6883. DOI: 10.2172/1665769. URL: https://www.osti.gov/servlets/purl/1665769/.

[43] Christian Træland. "Grid Tariffs for Fast Charging Stations in the Norwegian Distribution Grid". MA thesis. Trondheim: NTNU, 2020.

[44] Rajab Khalilpour and Anthony Vassallo. "Planning and operation scheduling of PV-battery systems: A novel methodology". In: *Renewable and Sustainable Energy Reviews* 53 (Jan. 1, 2016), pp. 194–208. ISSN: 1364-0321. DOI: 10.1016/j.rser.2015.08.015.

[45] Jizhong Zhu. "OPTIMIZATION OF POWER SYSTEM OPERATION". In: (2009), p. 623.

[46] Nan Qin. *Voltage Control in the Future Power Transmission Systems*. Springer Theses. Cham: Springer International Publishing, 2018. DOI: 10.1007/978-3-319-69886-1.

[47] Adam Kierad. *Load flow (power flow) - step-by-step, theory and calculation*. Electrism. URL: https://electrisim.com/load-flow-power-flow.html.

[48] Morris Brenna et al. "Voltage Control in Smart Grids: An Approach Based on Sensitivity Theory". In: *Journal of Electromagnetic Analysis and Applications* 02.8 (2010), pp. 467–474. ISSN: 1942-0730, 1942-0749. DOI: 10.4236/jemaa.2010.28062.

[49] B. Bakhshideh Zad et al. "Optimal reactive power control of DGs for voltage regulation of MV distribution systems using sensitivity analysis method and PSO algorithm". In: *International Journal of Electrical Power & Energy Systems* 68 (June 1, 2015), pp. 52–60. ISSN: 0142-0615. DOI: 10.1016/j.ijepes.2014.12.046.

[50] Fabrizio Pilo, Giuditta Pisano, and Gian Giuseppe Soma. "Optimal Coordination of Energy Resources With a Two-Stage Online Active Management". In: *IEEE Transactions on Industrial Electronics* 58.10 (Oct. 2011). Conference Name: IEEE Transactions on Industrial Electronics, pp. 4526–4537. ISSN: 1557-9948. DOI: 10.1109/TIE.2011.2107717.

[51] Gustavo Valverde and Thierry Van Cutsem. "Model Predictive Control of Voltages in Active Distribution Networks". In: *IEEE Transactions on Smart Grid* 4.4 (Dec. 2013). Conference Name: IEEE Transactions on Smart Grid, pp. 2152–2161. ISSN: 1949-3061. DOI: 10.1109/TSG.2013.2246199.

[52] M. Farina et al. "Model predictive control of voltage profiles in MV networks with distributed generation". In: *Control Engineering Practice* 34 (Jan. 1, 2015), pp. 18–29. ISSN: 0967-0661. DOI: 10.1016/j.conengprac.2014.09.010.

[53] Yimy E. García Vera, Rodolfo Dufo-López, and José L. Bernal-Agustín. "Energy Management in Microgrids with Renewable Energy Sources: A Literature Review". In: *Applied Sciences* 9.18 (Sept. 13, 2019), p. 3854. ISSN: 2076-3417. DOI: 10.3390/app9183854.

[54] Chun Sing Lai et al. "Levelized cost of electricity for photovoltaic/biogas power plant hybrid system with electrical energy storage degradation costs". In: *Energy Conversion and Management* 153 (Dec. 1, 2017), pp. 34–47. ISSN: 0196-8904. DOI: 10.1016/j.enconman.2017.09.076.

[55] Richard Bean and Hina Khan. "Using solar and load predictions in battery scheduling at the residential level". In: (Oct. 25, 2018). URL: http://arxiv.org/abs/1810.11178.

[56] Elizabeth L. Ratnam, Steven R. Weller, and Christopher M. Kellett. “An optimization-based approach to scheduling residential battery storage with solar PV: Assessing customer benefit”. In: *Renewable Energy* 75 (Mar. 1, 2015), pp. 123–134. ISSN: 0960-1481. DOI: 10.1016/j.renene.2014.09.008.

[57] Nina Lindholm. “Islanded Microgrids: a Predictive Approach to Control Operation”. In: (June 2020), p. 80.

[58] T. Lepold and D. Georges. “Energy management system for charging stations with regenerative supply and battery storage based on hybrid model predictive control”. In: *2017 IEEE Conference on Control Technology and Applications (CCTA)*. 2017 IEEE Conference on Control Technology and Applications (CCTA). Aug. 2017, pp. 799–805. DOI: 10.1109/CCTA.2017.8062558.

[59] Ibán JUNQUERA MARTÍNEZ et al. “Energy management of micro renewable energy source and electric vehicles at home level”. In: *Journal of Modern Power Systems and Clean Energy* 5.6 (Nov. 1, 2017), pp. 979–990. ISSN: 2196-5420. DOI: 10.1007/s40565-017-0326-8.

[60] Dennis van der Meer et al. “Energy Management System with PV Power Forecast to Optimally Charge EVs at the Workplace”. In: *IEEE Transactions on Industrial Informatics* PP (Dec. 1, 2016), pp. 1–1. DOI: 10.1109/TII.2016.2634624.

[61] Jose Luis Torres-Moreno et al. “Energy Management Strategy for Micro-Grids with PV-Battery Systems and Electric Vehicles”. In: *Energies* 11.3 (Mar. 2018). Number: 3 Publisher: Multidisciplinary Digital Publishing Institute, p. 522. DOI: 10.3390/en11030522.

[62] Y. WU et al. “A Real Time Energy Management for EV Charging Station Integrated with Local Generations and Energy Storage System”. In: *2018 IEEE Transportation Electrification Conference and Expo (ITEC)*. 2018 IEEE Transportation Electrification Conference and Expo (ITEC). June 2018, pp. 1–6. DOI: 10.1109/ITEC.2018.8450235.

[63] F. Kazhamiaka, C. Rosenberg, and S. Keshav. “Practical Strategies for Storage Operation in Energy Systems: Design and Evaluation”. In: *IEEE Transactions on Sustainable Energy* 7.4 (Oct. 2016). Conference Name: IEEE Transactions on Sustainable Energy, pp. 1602–1610. ISSN: 1949-3037. DOI: 10.1109/TSTE.2016.2569425.

[64] *FASIT Kravspesifikasjon : versjon 2019*. SINTEF. URL: https://www.sintef.no/publikasjoner/publikasjon/.

[65] Eirik Ivarsøy. “Demand modeling of high-power electric vehicle charging”. In: (Dec. 2019), p. 61.

[66] *Historical Market Data*. Nord Pool. URL: https://www.nordpoolgroup.com/historical-market-data/.

[67] Eirik Ivarsoy, Bendik Nybakk Torsater, and Magnus Korpas. “Stochastic Load Modeling of High-Power Electric Vehicle Charging - A Norwegian Case Study”. In: *2020 International Conference on Smart Energy Systems and Technologies (SEST)*. 2020 International Conference on Smart Energy Systems and Technologies (SEST). Istanbul, Turkey: IEEE, Sept. 2020, pp. 1–6. ISBN: 978-1-72814-701-7. DOI: 10.1109/SEST48500.2020.9203102.

[68] Renate Høvik Berge, Fredrik Rudfoss Haugland, and Ida Erika Witt Langseth. "Optimization of Microgrids: Feasibility Study and Economic Analysis of Rye Microgrid". In: (2019). Accepted: 2019-06-30T14:00:22Z Publisher: NTNU. URL: https://ntnuopen.ntnu.no/ntnu-xmlui/handle/11250/2602893.

[69] L. Thurner et al. "pandapower — An Open-Source Python Tool for Convenient Modeling, Analysis, and Optimization of Electric Power Systems". In: *IEEE Transactions on Power Systems* 33.6 (Nov. 2018), pp. 6510–6521. ISSN: 0885-8950. DOI: 10.1109/TPWRS.2018.2829021.

[70] Eirik Ivarsøy. "Optimal planning of fast charging stations for EVs – A Norwegian case study". In: (June 2020), p. 106.

[71] NVE. *Forskrift om leveringskvalitet i kraftsystemet*. URL: https://lovdata.no/dokument/SF/forskrift/2004-11-30-1557#KAPITTEL_4.

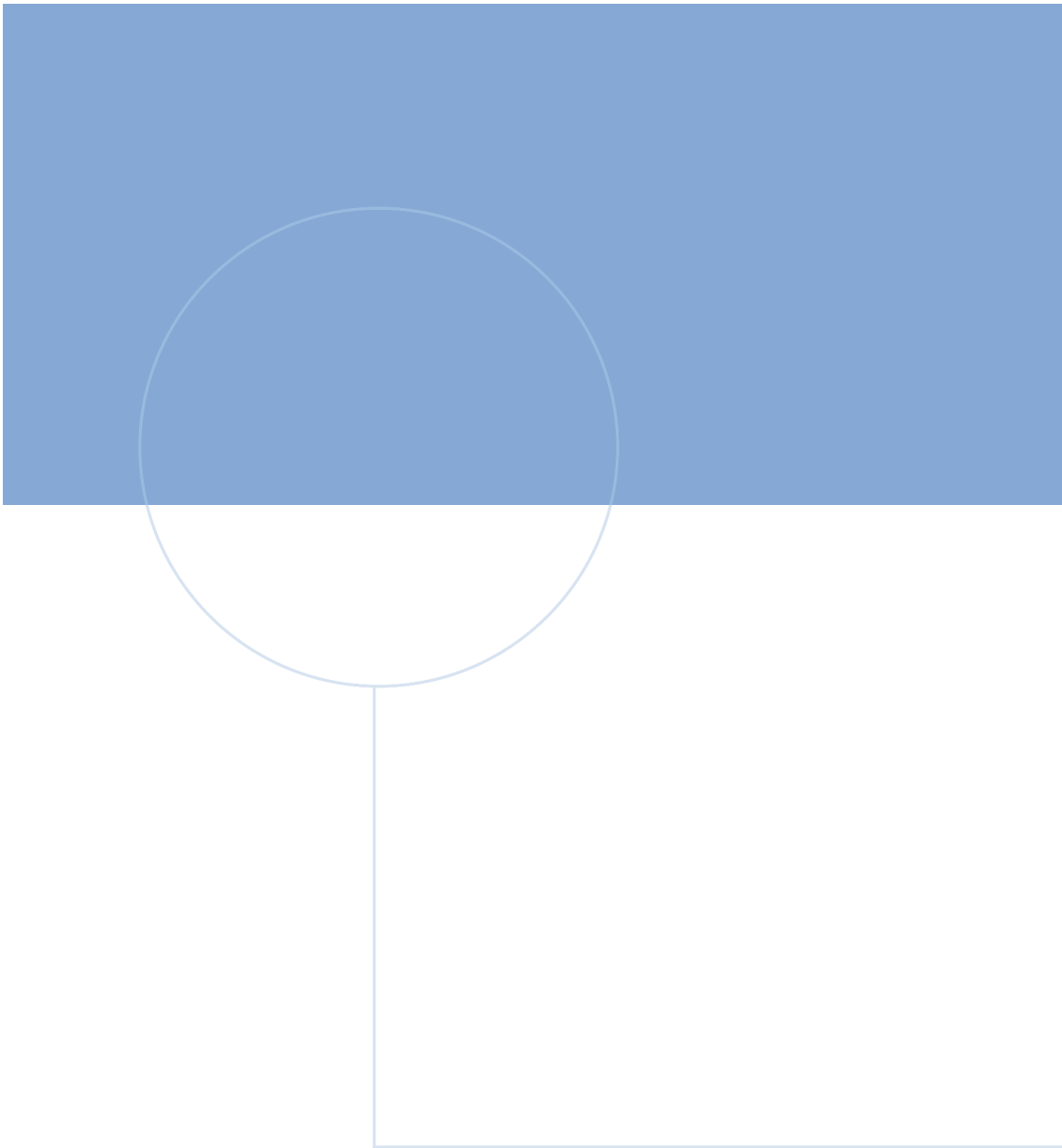

NTNU

Kunnskap for en bedre verden